Observations of flows in active-region loops: as a response to coronal heating

Hirohisa Hara
National Astronomical Observatory of Japan

2013 Jun 26

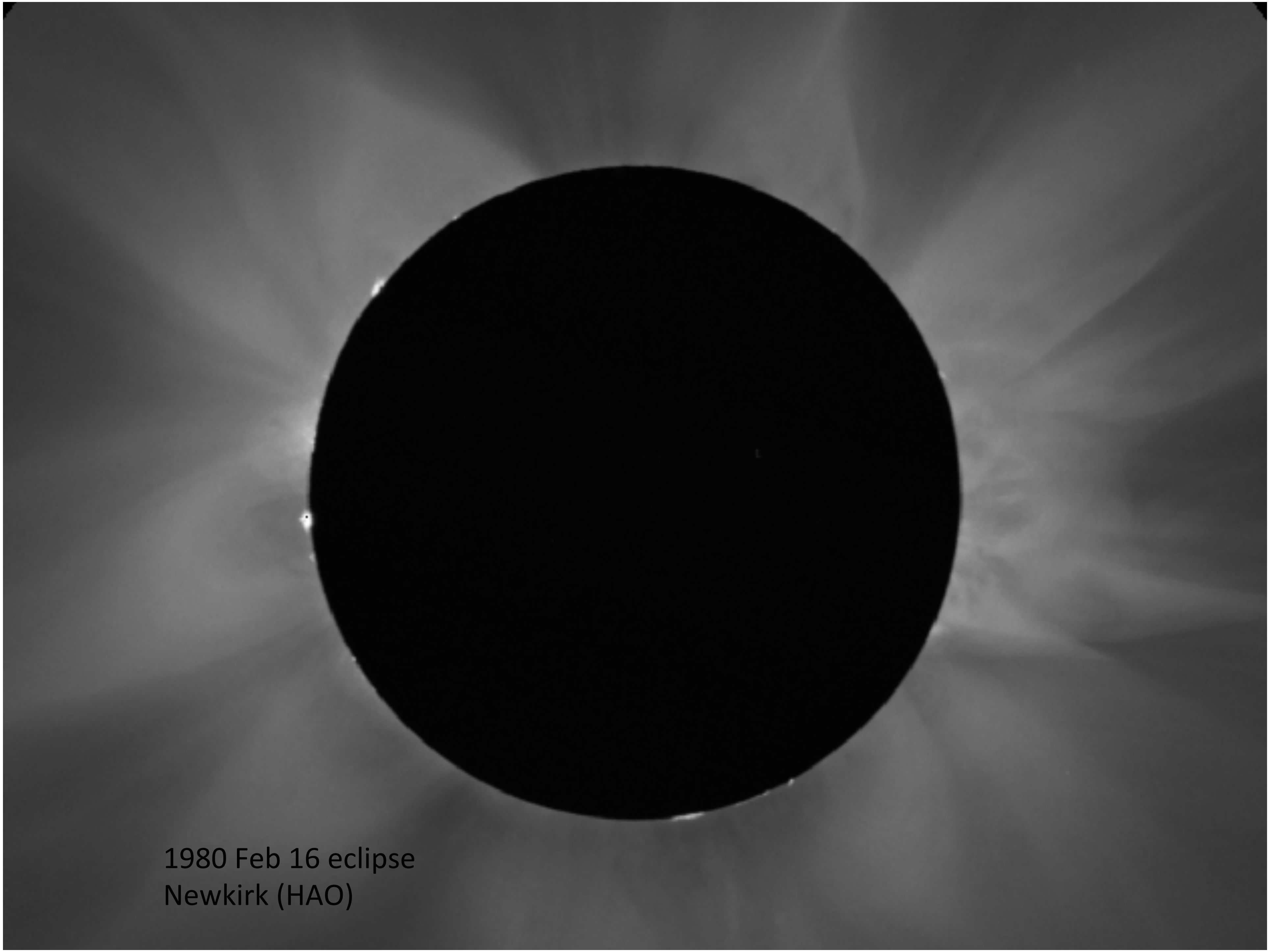
1980 Feb 16 eclipse
Newkirk (HAO)

Building blocks and radiative outputs

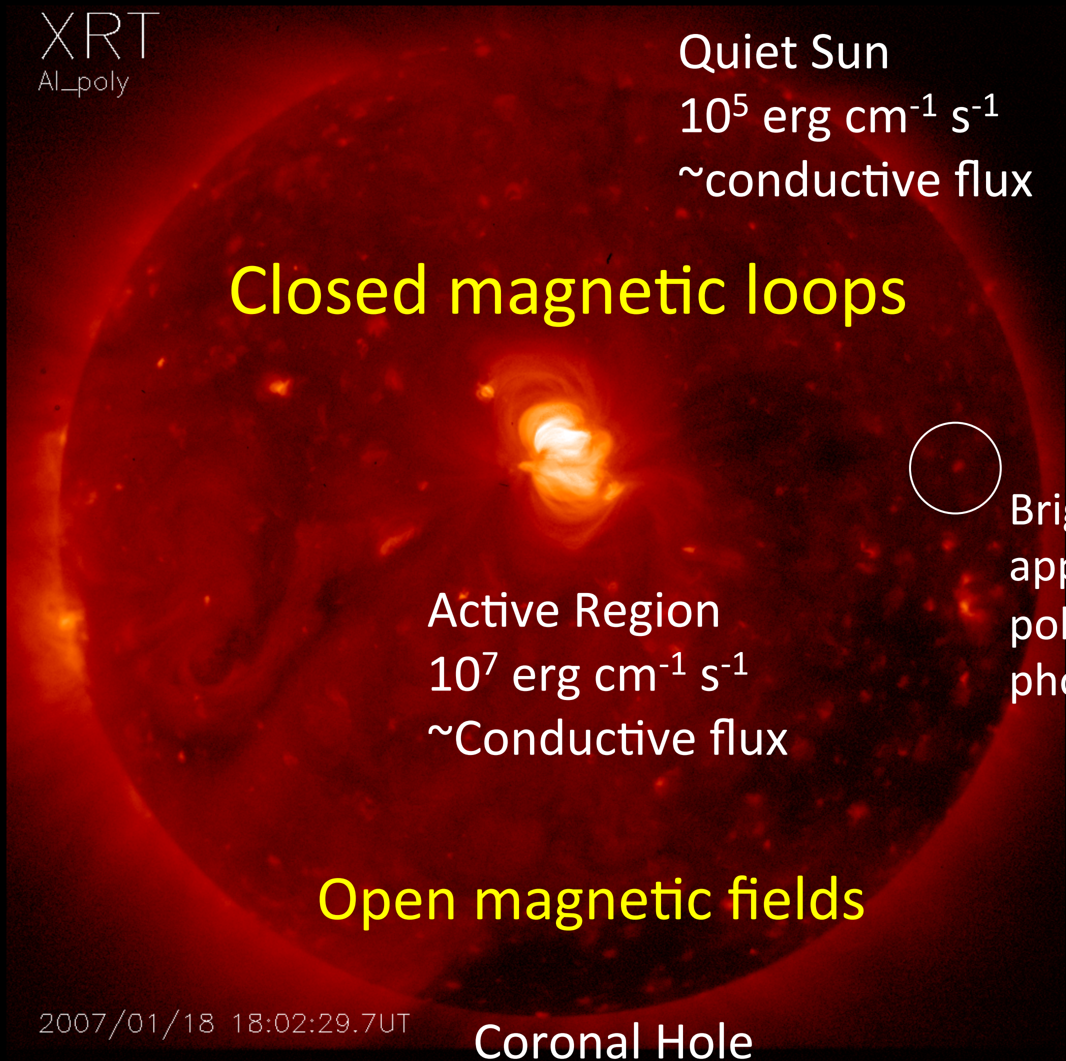

Quiet Sun
10^5 erg cm^{-1} s^{-1}
~conductive flux

Closed magnetic loops

Bright points:
appear above opposite polarity encounter at photosphere

Active Region
10^7 erg cm^{-1} s^{-1}
~Conductive flux

Open magnetic fields

Coronal Hole
10^4 erg cm^{-1} s^{-1}
<< conductive flux

Values from Withbroe & Noyes 1977

Analysis so far made

- Filter/line ratio temperature and density
  - To find a temperature gradient along a loop
  - Meaningless to multi-thread loop modelers?
- Differential emission measure
  - To compare the modeling results with observations
- Small amplitude intensity fluctuation
  - To find a signature of impulsive nanoflare-scale energy deposition at the coronal height
- High-speed upflow from spectroscopy
  - Response of coronal plasmas after heating occurs
- Detection of a type of waves by intensity and Doppler variations at multiple points
  - Estimating the wave energy flux in the corona
- Anisotropy of nonthermal broadening in coronal emission line
  - as tool to see the unresolved/fast wave signature

Doppler measurements of Flow speed before EIS

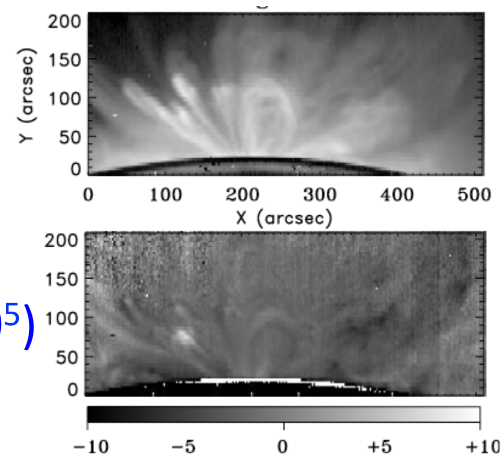

- Measurements during the total Eclipse and with ground-based coronagraphs
  - Almost lateral view to coronal loops, but high $\lambda/\Delta\lambda$ ~$O(10^5)$
- OSO & Skylab
  - Low spectral resolution for scanning instruments
  - Low spatial resolution to see loop structures for high $\lambda/\Delta\lambda$ instruments

    ➔ Average Doppler speed in quiet-Sun TR and corona
- SERTS sounding rocket flight
  - Sensitivity of early flights was not enough to scan the field during a few min flight.
- SOHO
  - CDS: not easy to detect |v|<10 km/s due to broad instrumental width

    ➔ But, it measured spatially resolved chromospheric evaporation.
  - SUMER: has potential to investigate AR loops with enough $\lambda/\Delta\lambda$, but AR not frequently observed to avoid detector degradation by strong EUV

    ➔ Doppler map of QS & CH in a good spatial sampling was obtained.

Doppler Motion in AR Corona

- 10 km/s upflows in the active region corona have been reported in a SUMER observation (Teriaca et al. 1999).
- 5-20 km/s projected upflow speed has been reported in a TRACE imaging observation (Winebarger et al. 2001).
- High-precision 2D Doppler measurements over AR in the corona with EIS are new.

SUMER Slit pos. on EIT image

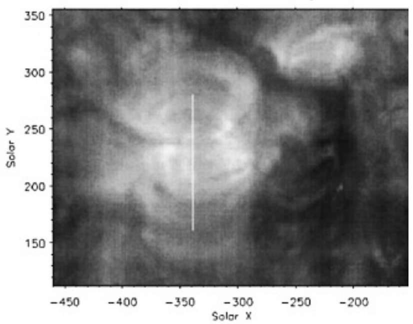

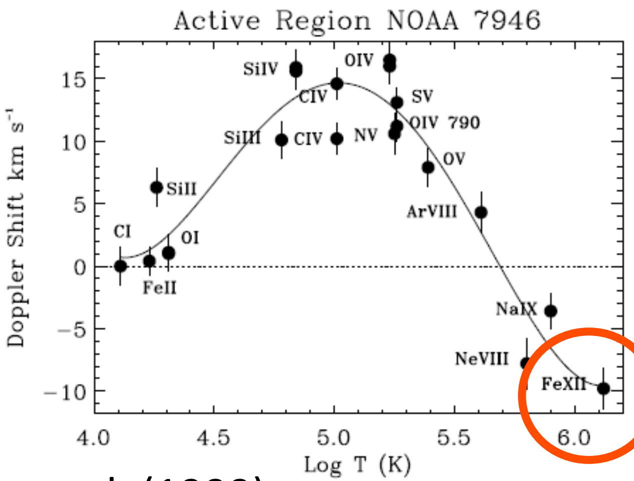

red

blue

Teriaca et al. (1999)

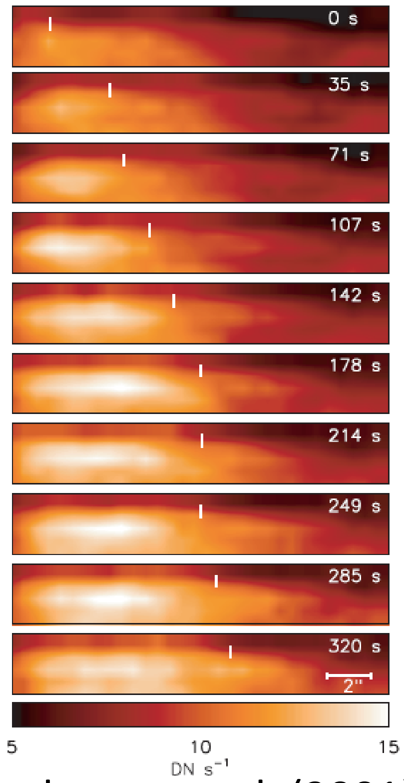

Winebarger et al. (2001)

EIS

- Design philosophy(1993; 20 years ago!):
  - To investigate TR & coronal dynamics by Doppler and line width measurement (but, $\lambda/\Delta\lambda \sim 4000$)
  - High sensitivity for short integration time
  - Simultaneous observations of a wide temperature range
- Approach for heating of coronal loops
  - High-resolution radiance map of a wide temperature range
    - N_e measurement along coronal loops
    - T_e measurement along coronal loops
  - Doppler & line broadening
    - Detection of waves in coronal loops
    - Flow along coronal loops
    - Detection of reconnection related flows
    - Turbulence

Instrument size

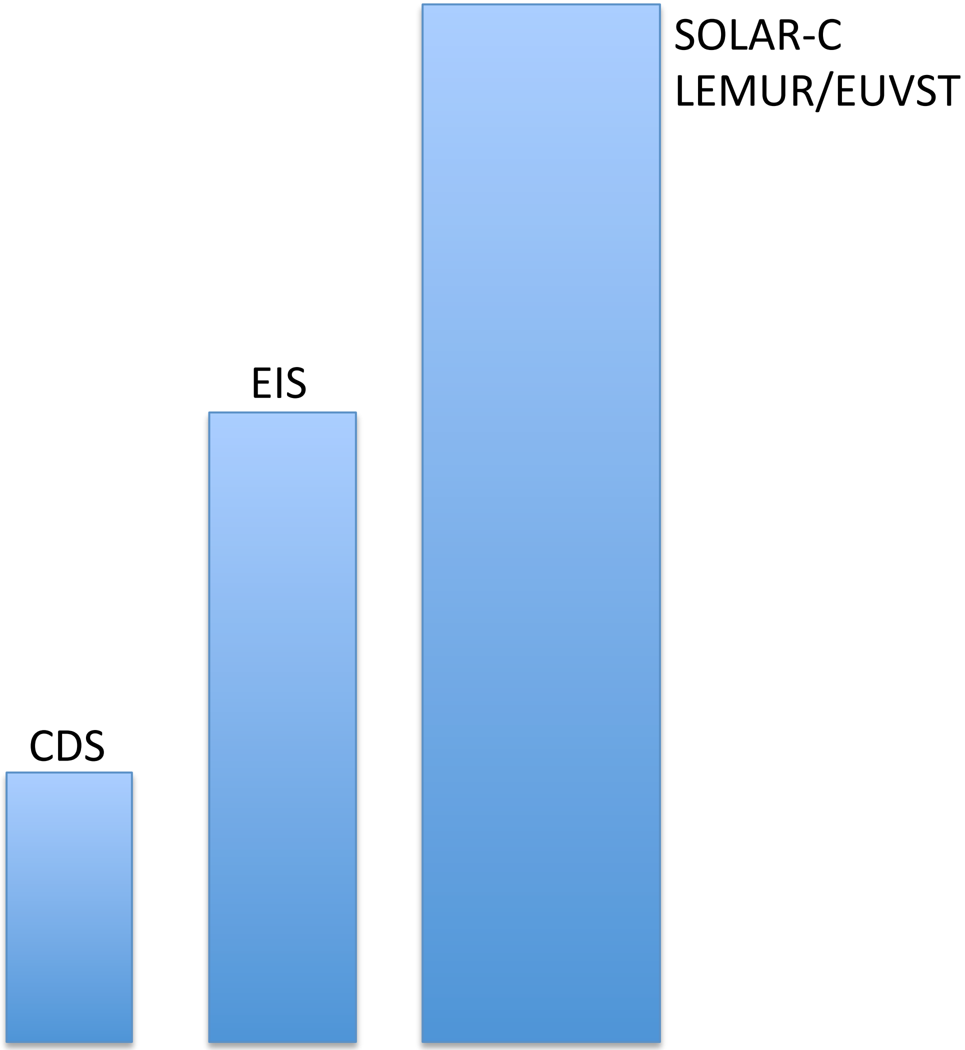

Basic Observables

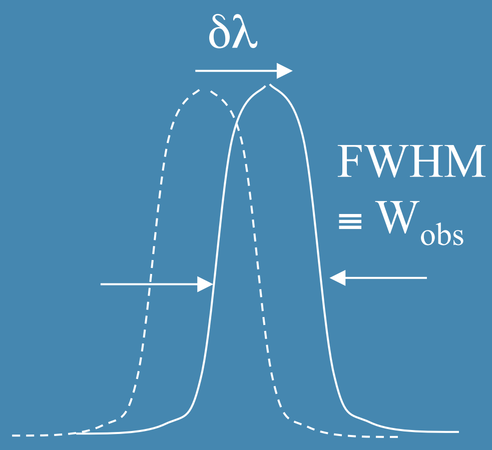

Information from a single emission line

- Line intensity
- Line shift by Doppler motion

  Doppler velocity = (δλ/λ) c
- Line width: temperature, non-thermal motion

thermal Doppler velocity

Instrumental width

nonthermal velocity

$$W_{\rm obs} = \sqrt{{W_{\rm I}}^2 + 4\ln 2\left(\frac{2kT_i}{M_i} + {V_{\rm NT}}^2\right)} \equiv \sqrt{{W_{\rm I}}^2 + W^2}$$

In velocity unit

$V_{\rm NT}$: nearly isotropic.

QS: Chae et al. 1998 from SUMER

AR: Hara & Ichimoto 1999, above the limb by a coronagraph

Information from selected two line ratio

- Temperature in a narrow range
- Density

Line center drift

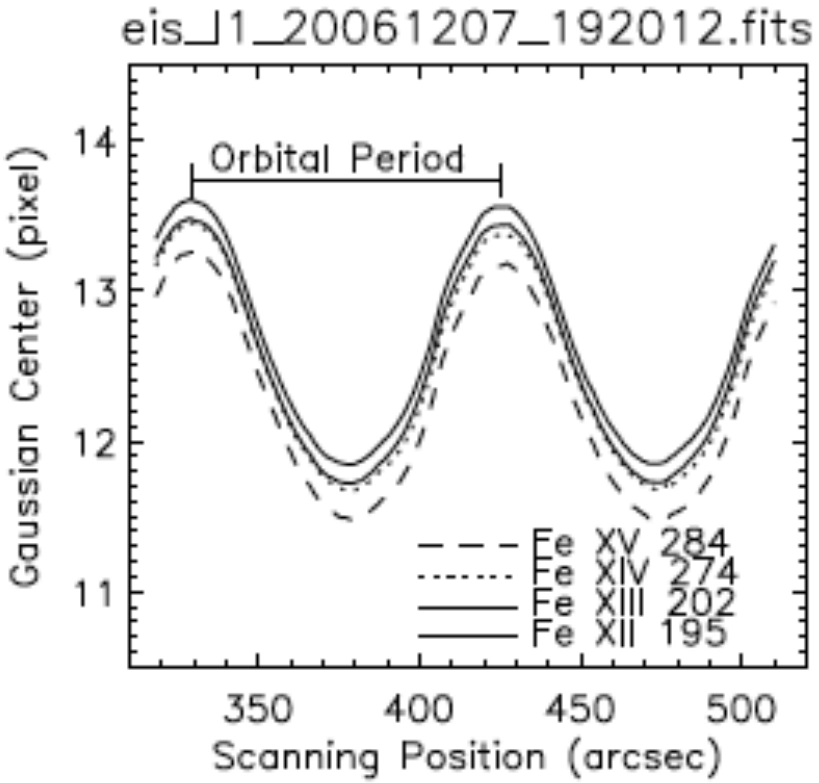

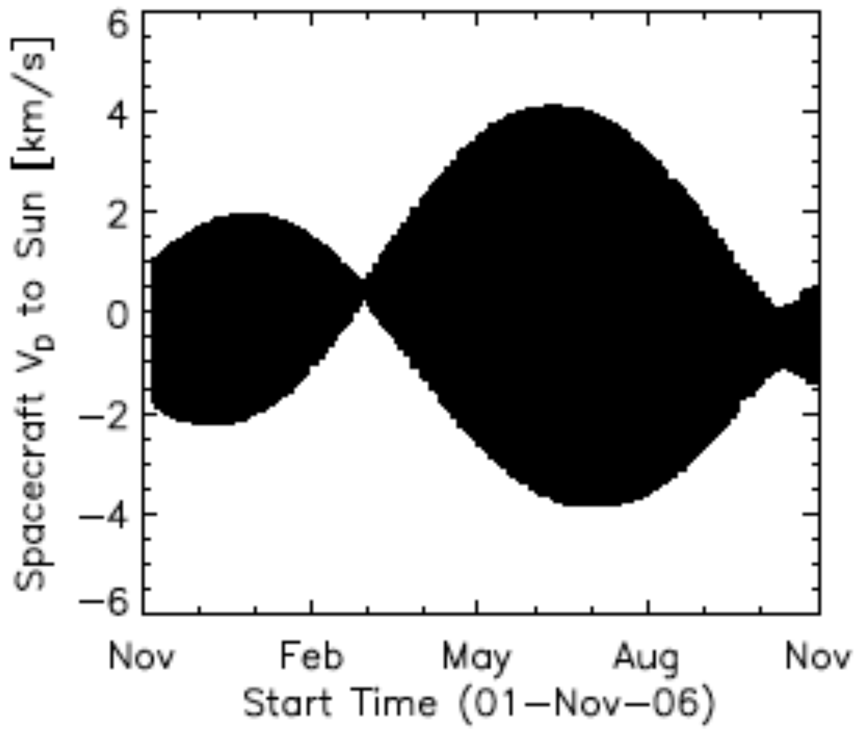

This can basically be detrended by a method in Kamio et al. 2010, Solar Phys. 266, 299.

Hara 2008, ASPC, 397,11

Equatorial fast QS scan

Fe II 195 Radiance(QS average)

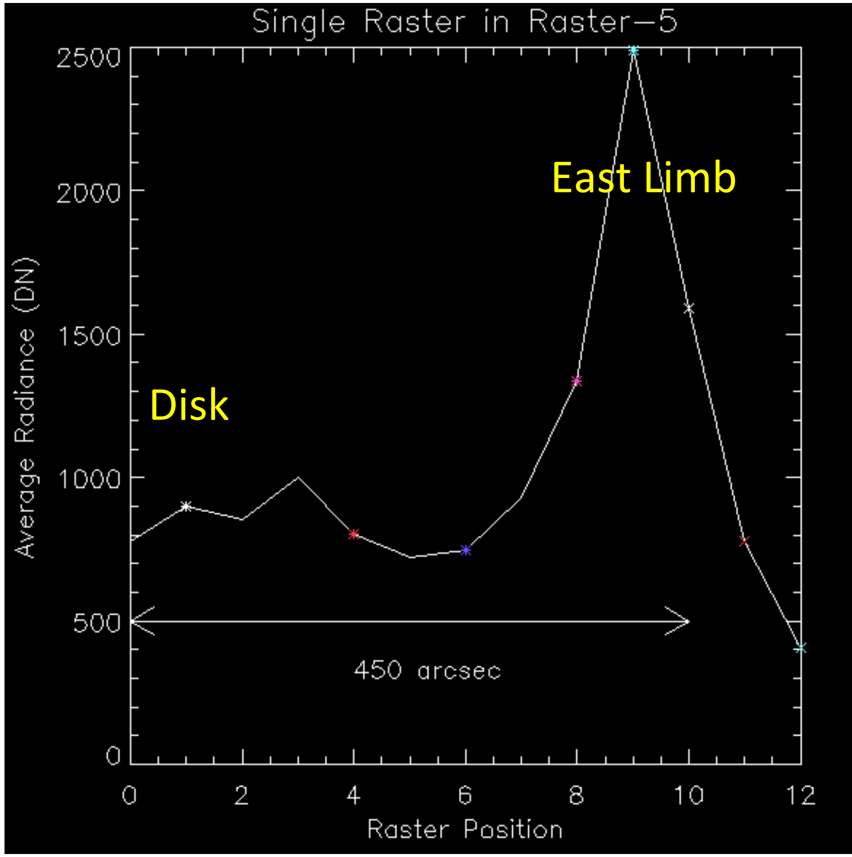

Fe II 195 line center

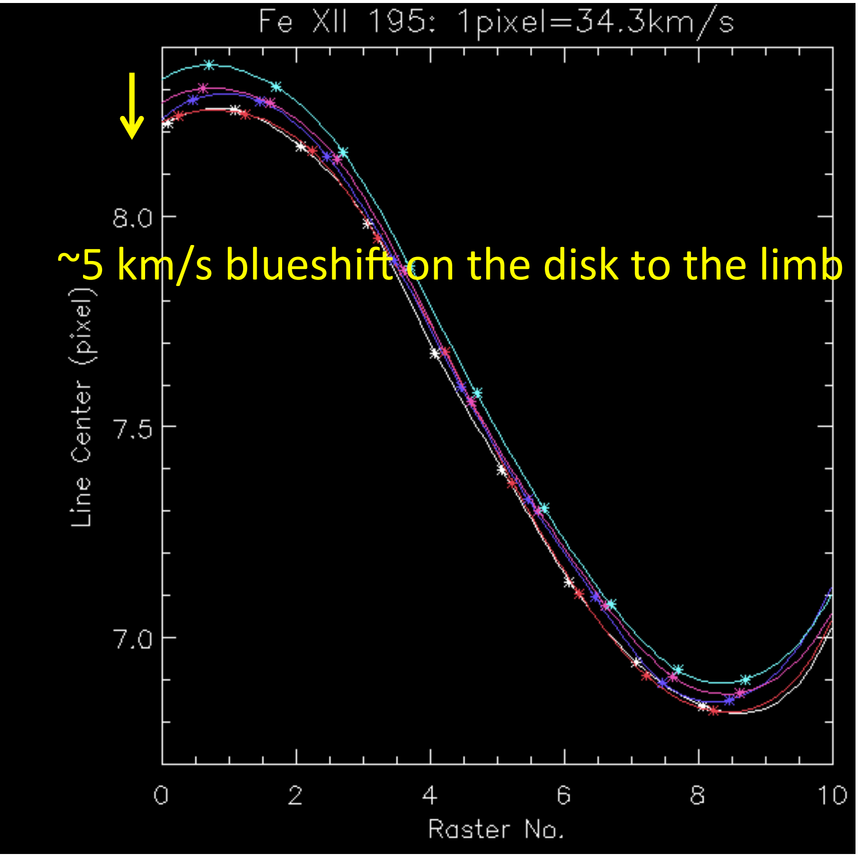

Personal expectation before starting EIS observations

- Upflow along coronal loops to fill magnetic loop structures
- High-speed flows as reconnection outflow from nanoflare magnetic structures
- Faint hot flows at the beginning of energy release
- Emerging loop structures in Doppler map

- Weak anisotropy of V_{NT} component（$\Delta V_{\mathrm{NT}} < 5\mathrm{km/s}$ in $V_{\mathrm{NT}} \sim 30\ \mathrm{km/s}$）in AR loops for a signature of Alfven wave
  - Hara & Ichimoto 1999, ApJ, 513, 969

Active Region (AR) flow map

- Doppler map of AR ~1km/s precision
  Doschek et al. (2007), Del Zanna (2008)
  Hara et al. (2008) etc.

- Doschek et a. (2007)
  - Enhanced line width at the edge of AR.
  - Line centroid correlate well with the width.
  - Other interesting features reported

- Del Zanna (2008)
  - T_e dependence of line shift relative to QS
    - Redshift in loop
    - Blueshift at the AR boundary

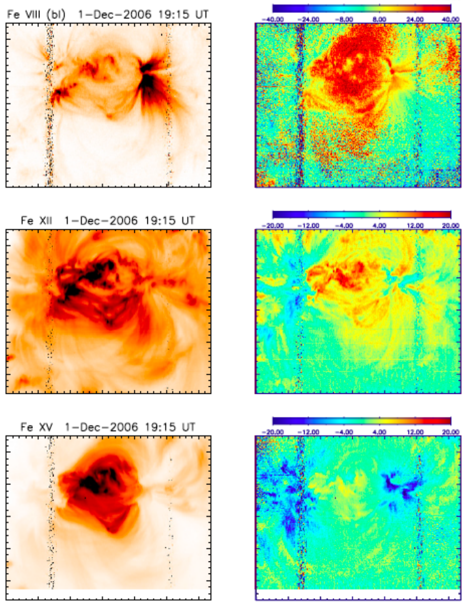

Del Zanna (2008)

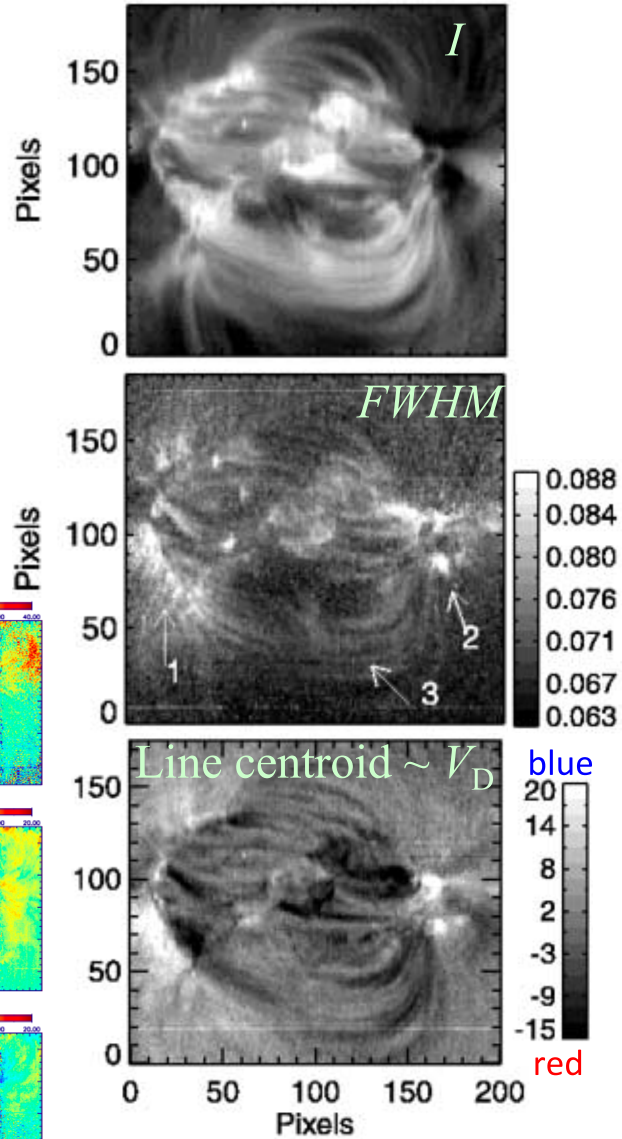

Doschek et al. (2007)

Maps from a Gaussian Fitting

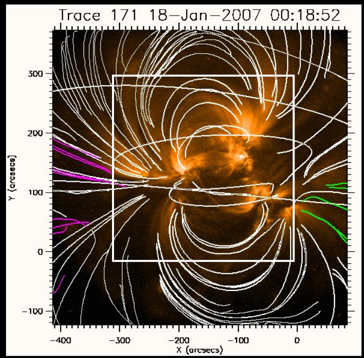

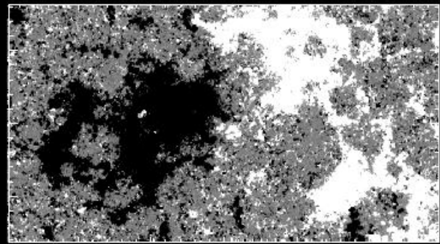

SOT SP
$B_{//}$

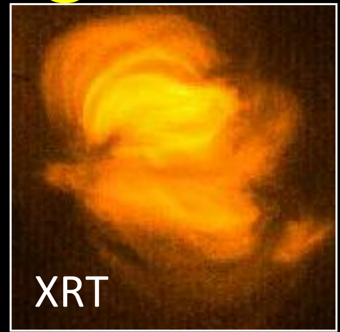

Fe XV 284 (log T = 6.3)

Scanning direction (= time)

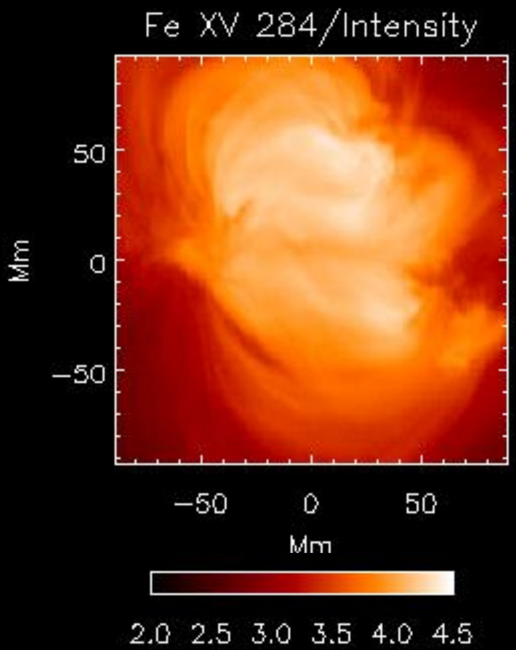

log I (photons)

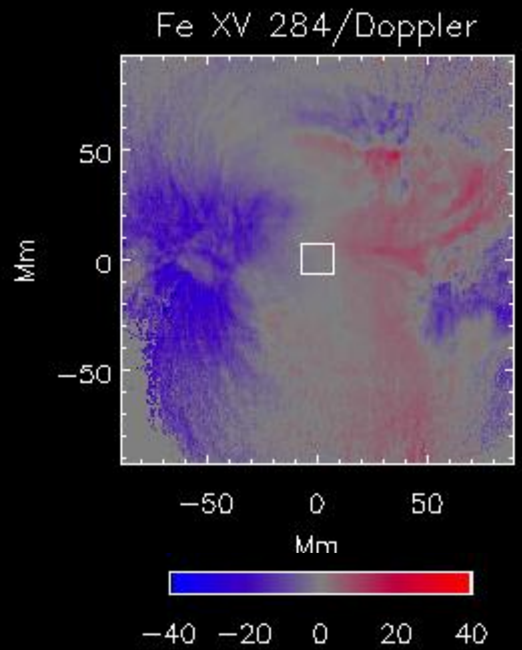

V_D (km/s)

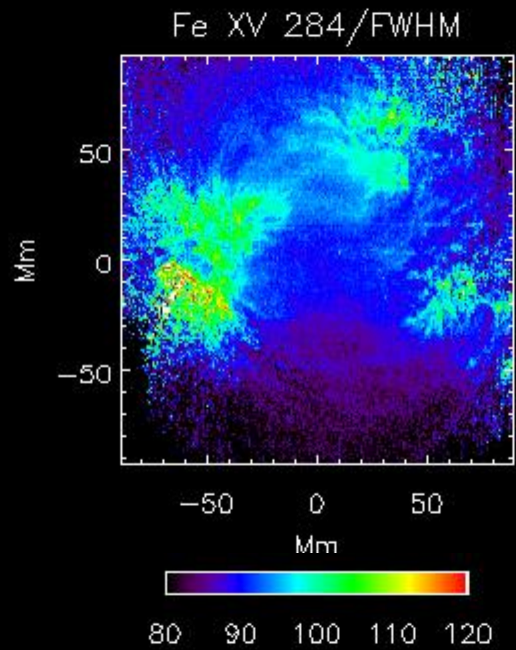

W_{OBS} (km/s)

Containing line broadening of instrumental origin

- Selection of AR: almost no microflares in GOES X-rays (~A-class)
- Selection of lines: similar structure to soft X-ray image containing hot loops

Maps from a Gaussian Fitting

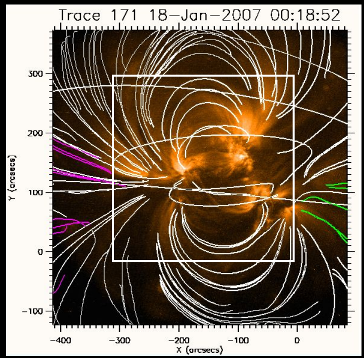

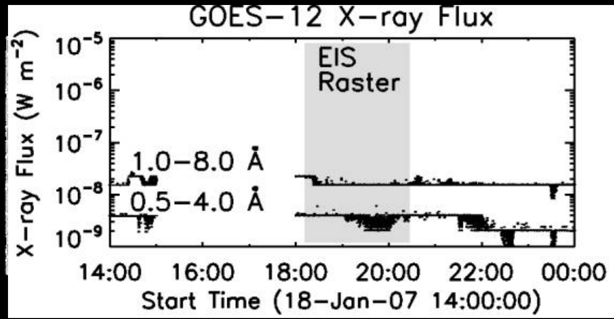

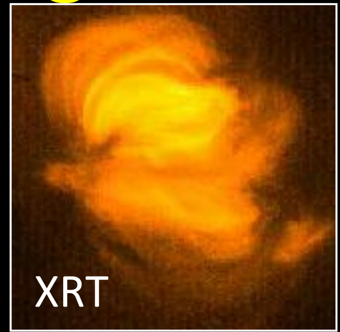

Fe XV 284 (log T = 6.3)

Scanning direction (= time)

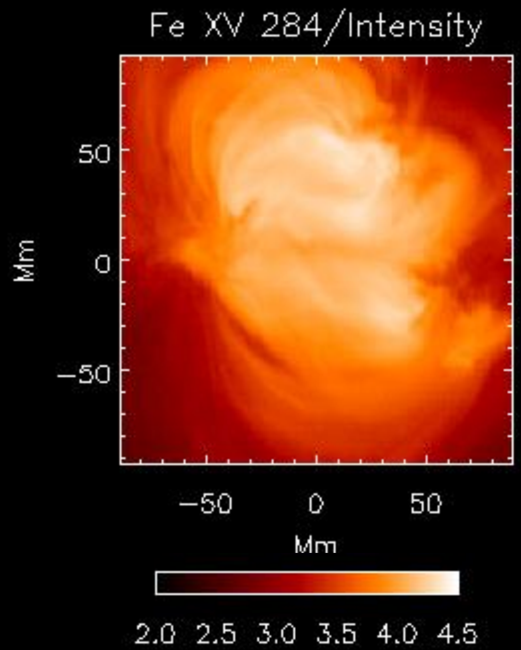

log I (photons)

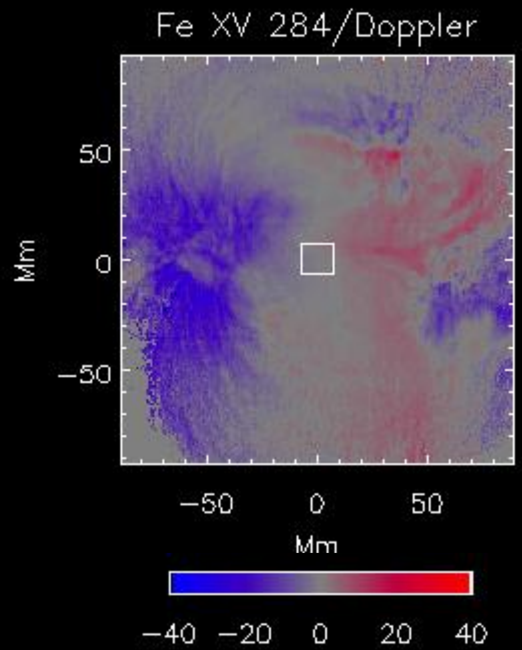

V_D (km/s)

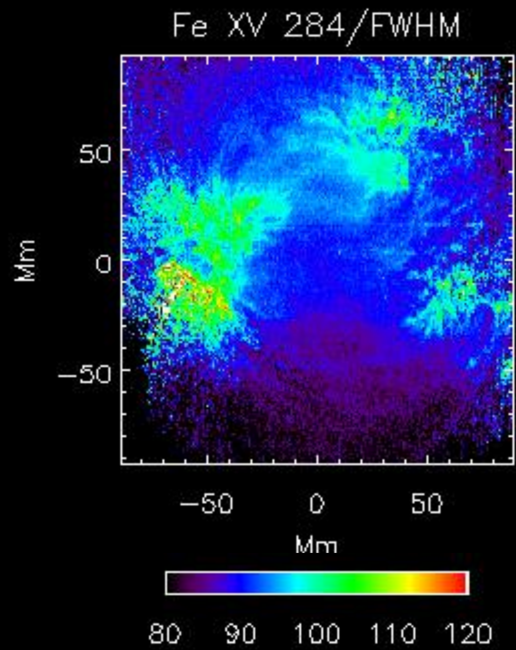

W_{OBS} (km/s)

Containing line broadening of instrumental origin

- Selection of AR: almost no microflares in GOES X-rays (~A-class)
- Selection of lines: similar structure to soft X-ray image containing hot loops

Height of FWHM enhancement

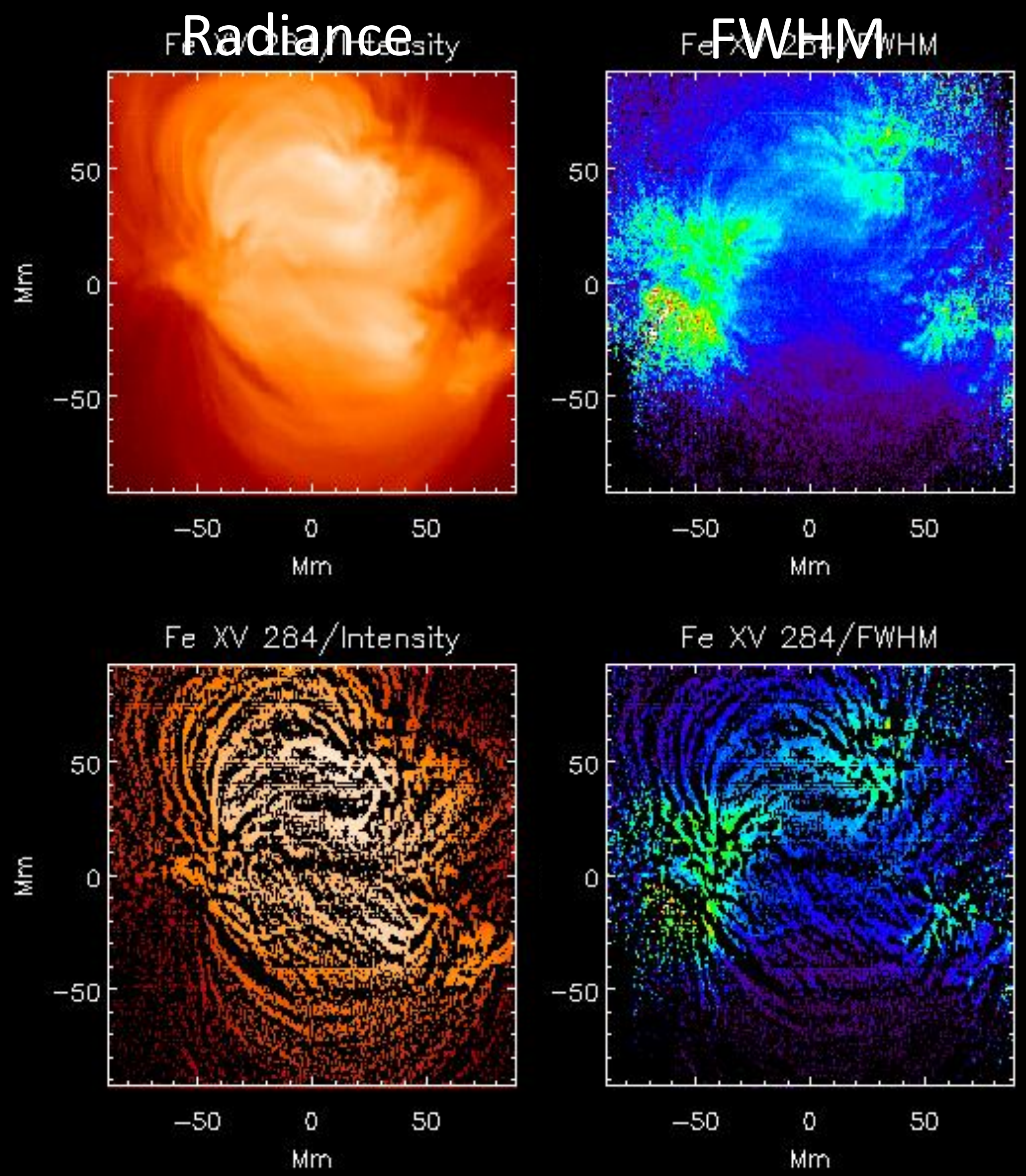

- A filter to find coronal loops is applied.
- Apparently FWHM decreases from the bottom to top in coronal loops.
- The scale length in the FWHM change ~ 10-20 Mm ?

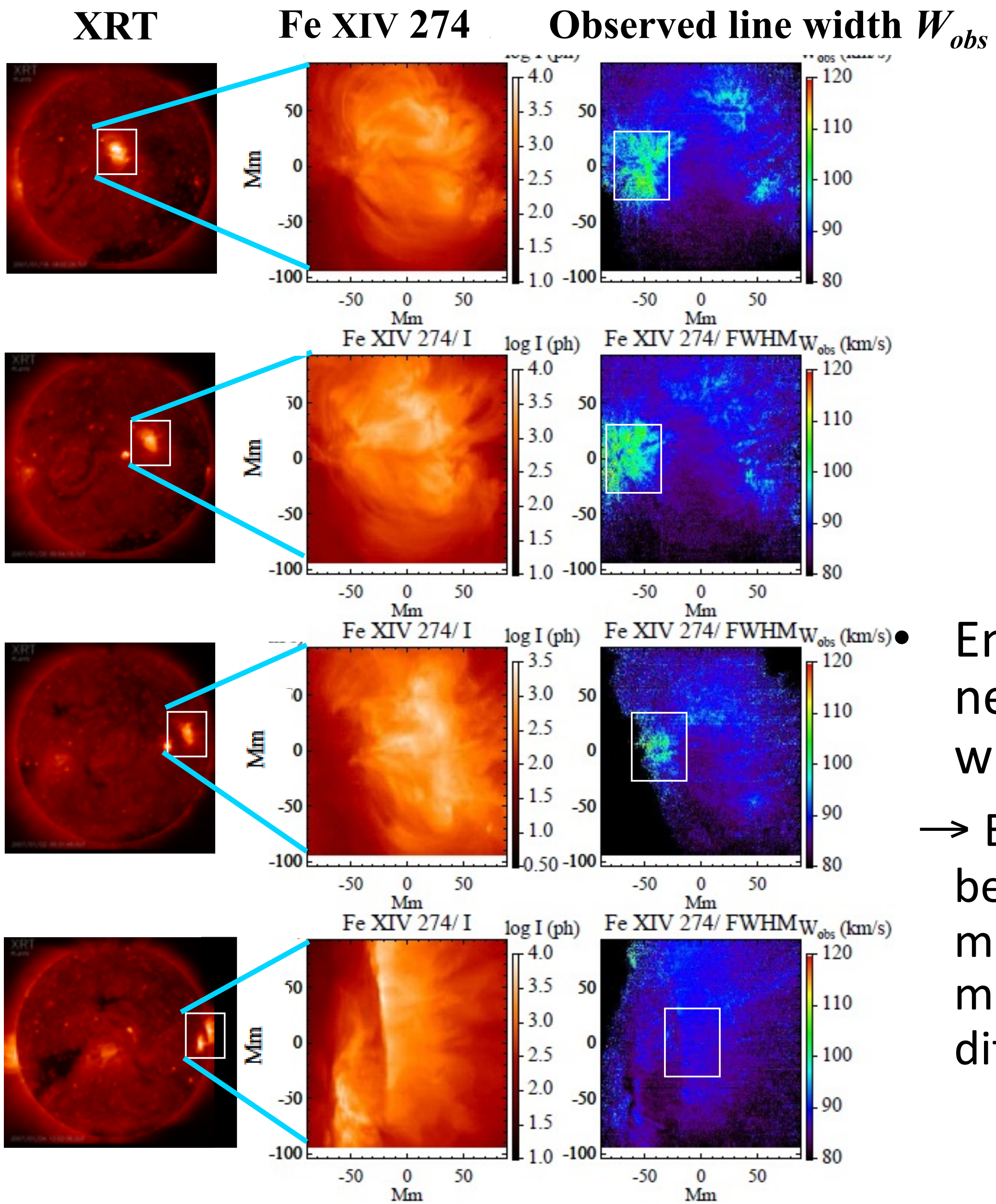

Line width change with rotation

- Enhanced line broadening near footpoints disappears with rotation.

→ Excess line broadening may be due to superposition of multiple components along magnetic field line, each with different line centers.

Center-to-limb Variation of motion near footpoints

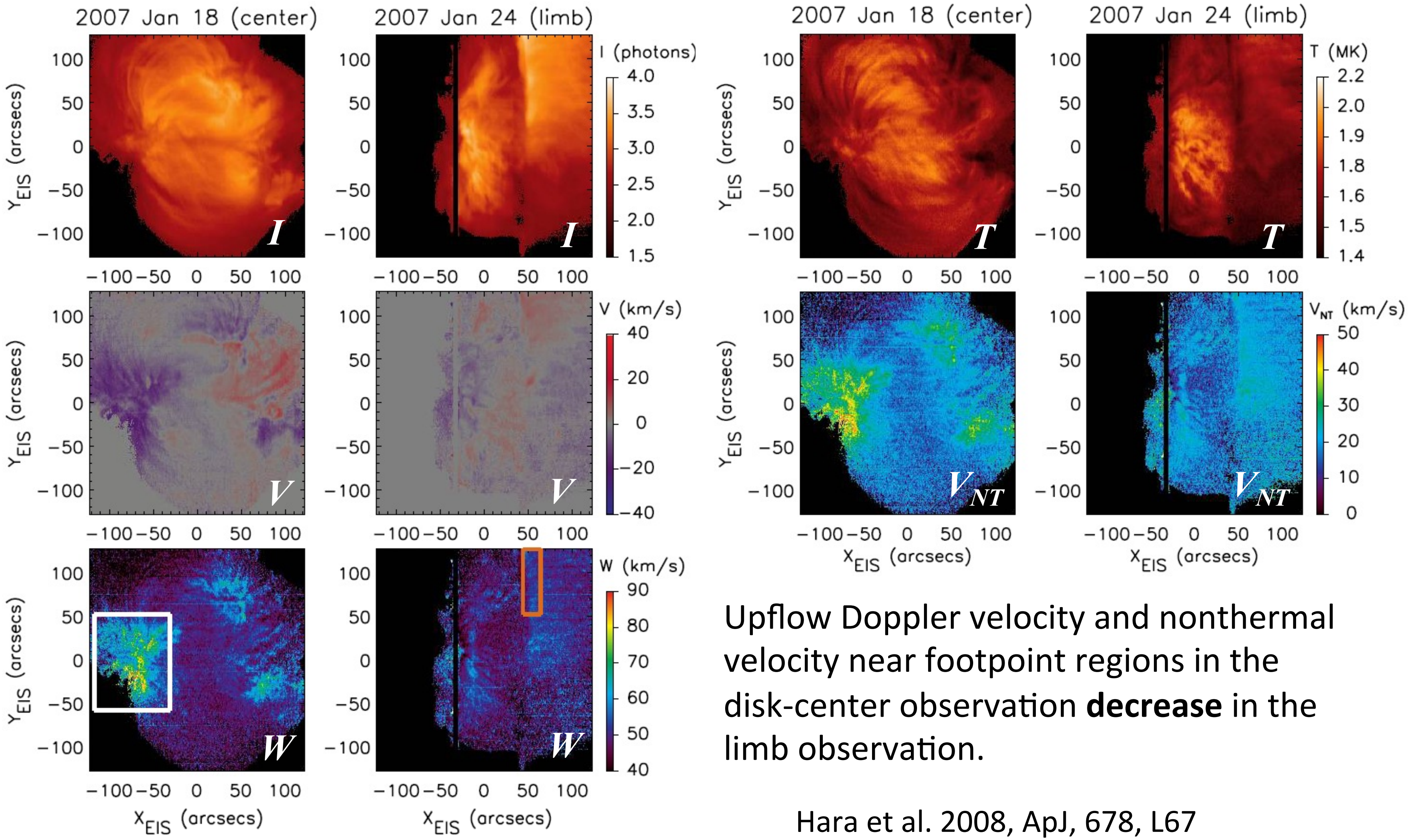

Upflow Doppler velocity and nonthermal velocity near footpoint regions in the disk-center observation **decrease** in the limb observation.

Hara et al. 2008, ApJ, 678, L67

Property of Flows

Histograms

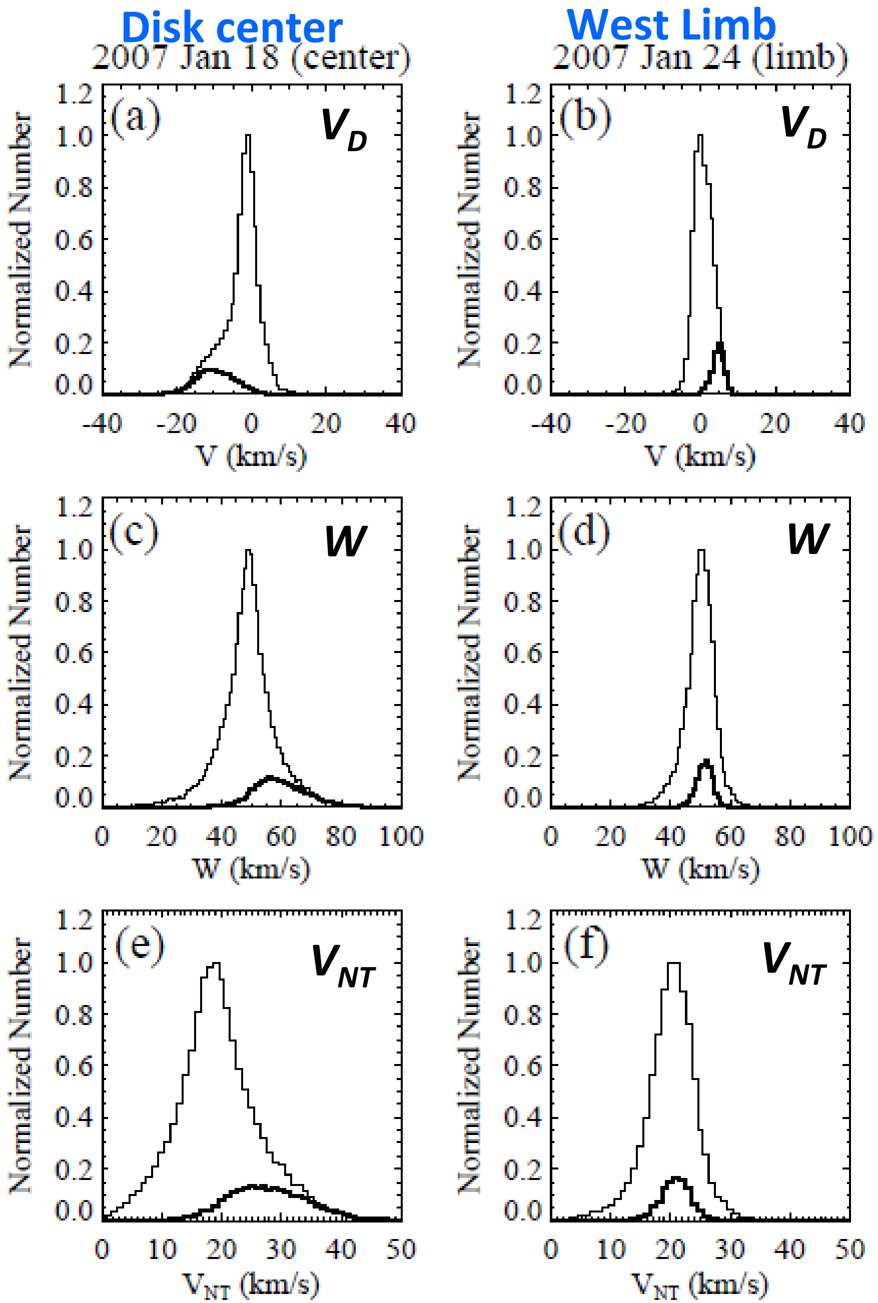

Fe XIV 274 V_{NT} map

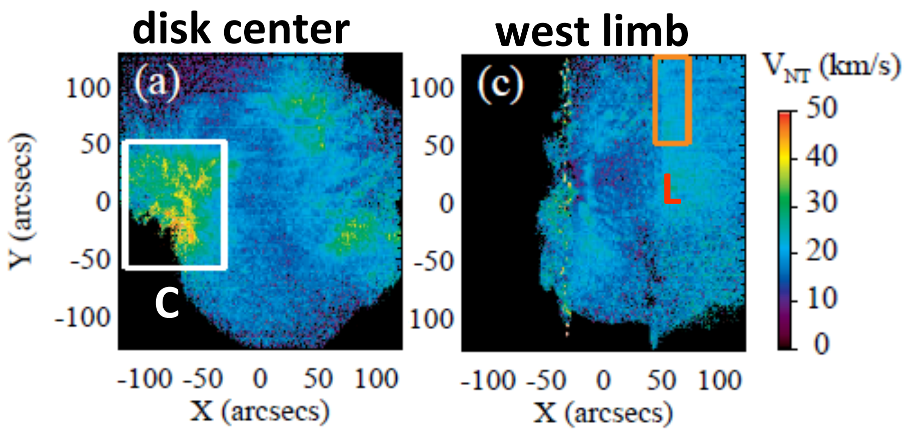

C: disk center **L**: limb

V_D : Doppler velocity
W : FWHM (instrumental width subtracted)
V_{NT} : Nonthermal velocity
(thermal width subtracted)

Thin lines : in whole FOV
Thick lines: in footpoint regions within square

Unresolved Flows

hidden in line width

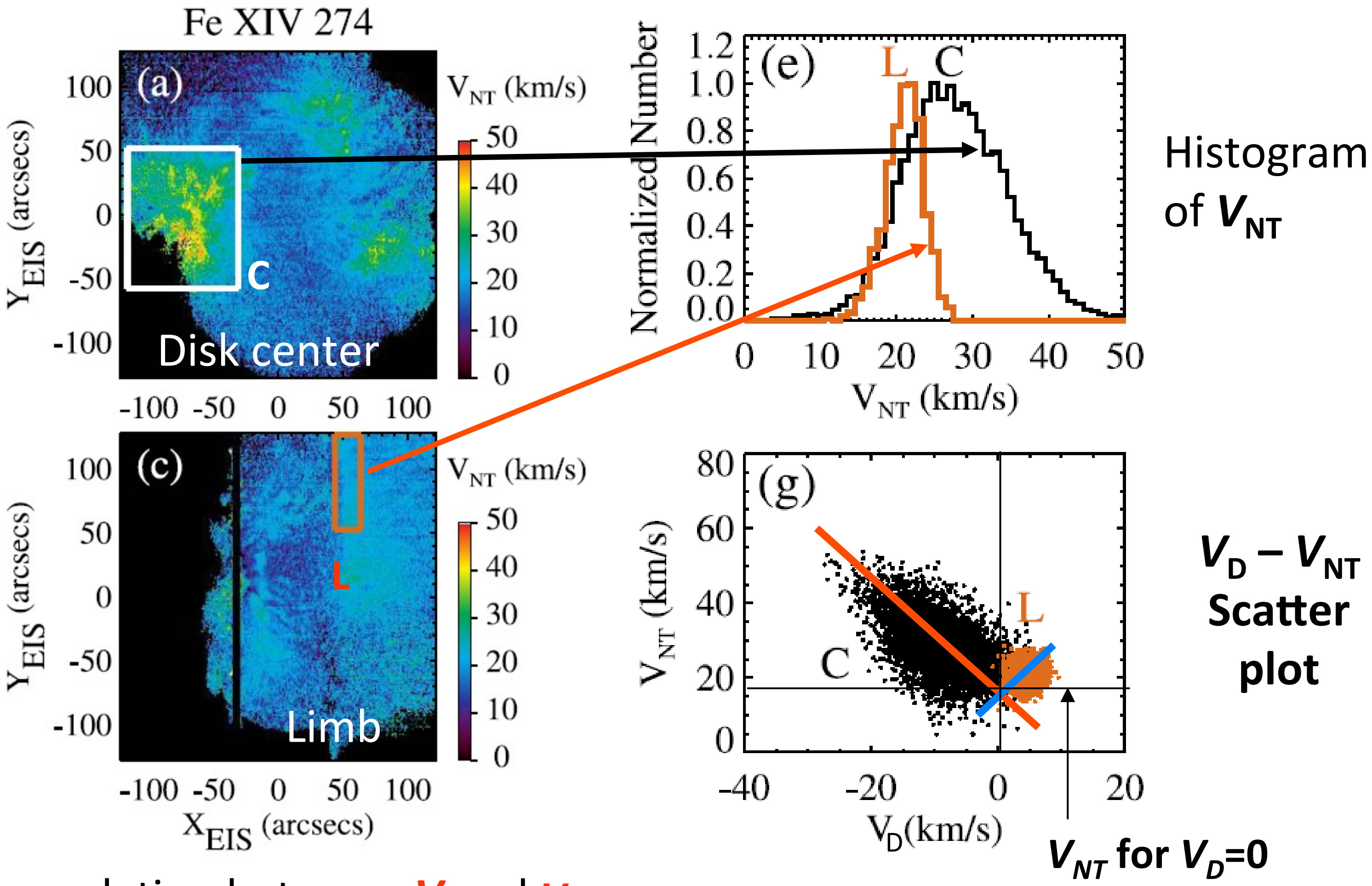

There is correlation between ***V*** and V_{NT}.

→ Superposition of line-of-sight plasma motions along magnetic field lines

Unresolved Doppler components are hidden !

Hara et al. 2008, ApJ, 678, L67

Multiple emission-line components

V_{NT} = 15.4 km/s

V_D = 10.5 km/s observed

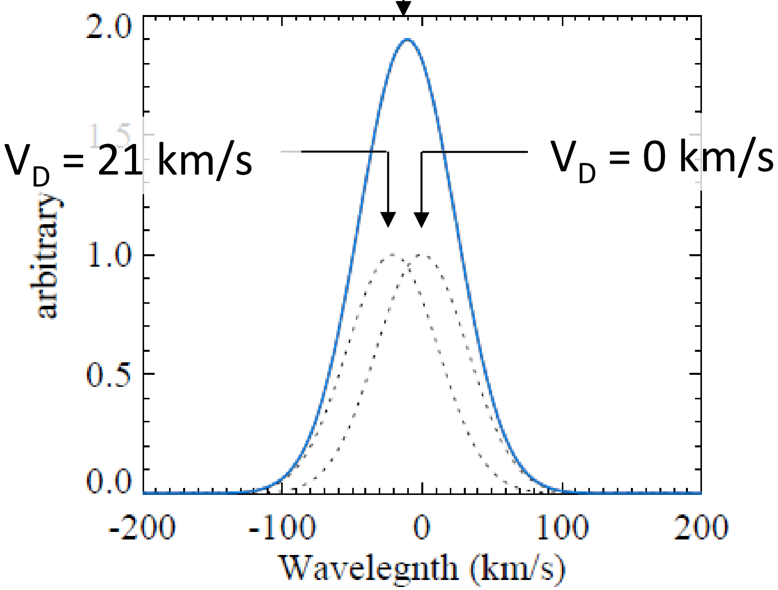

Two components model
with the same profile
as the simplest case

V_{NT} = 15.6 km/s

V_D = 12.9 km/s observed

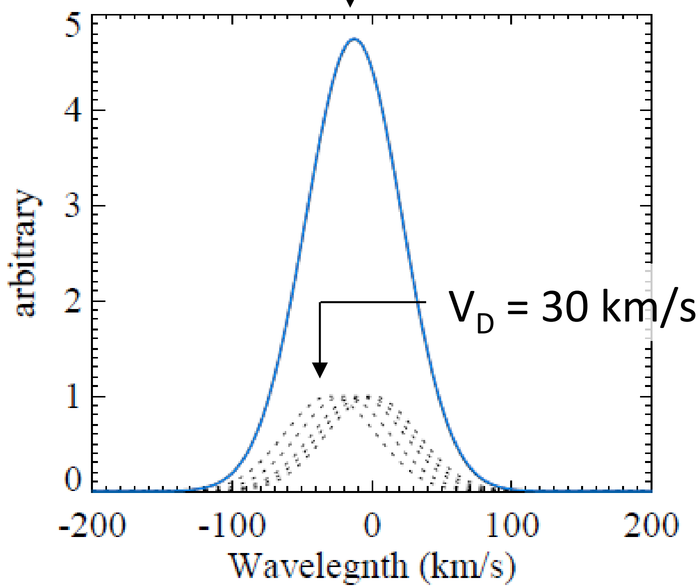

Blue lines: Gaussian-fitted line

Still a few tens of km/s

Blue-side Enhanced Line Profile

Line profiles at loop footpoints

This type of profile is found ubiquitously over the plage region.

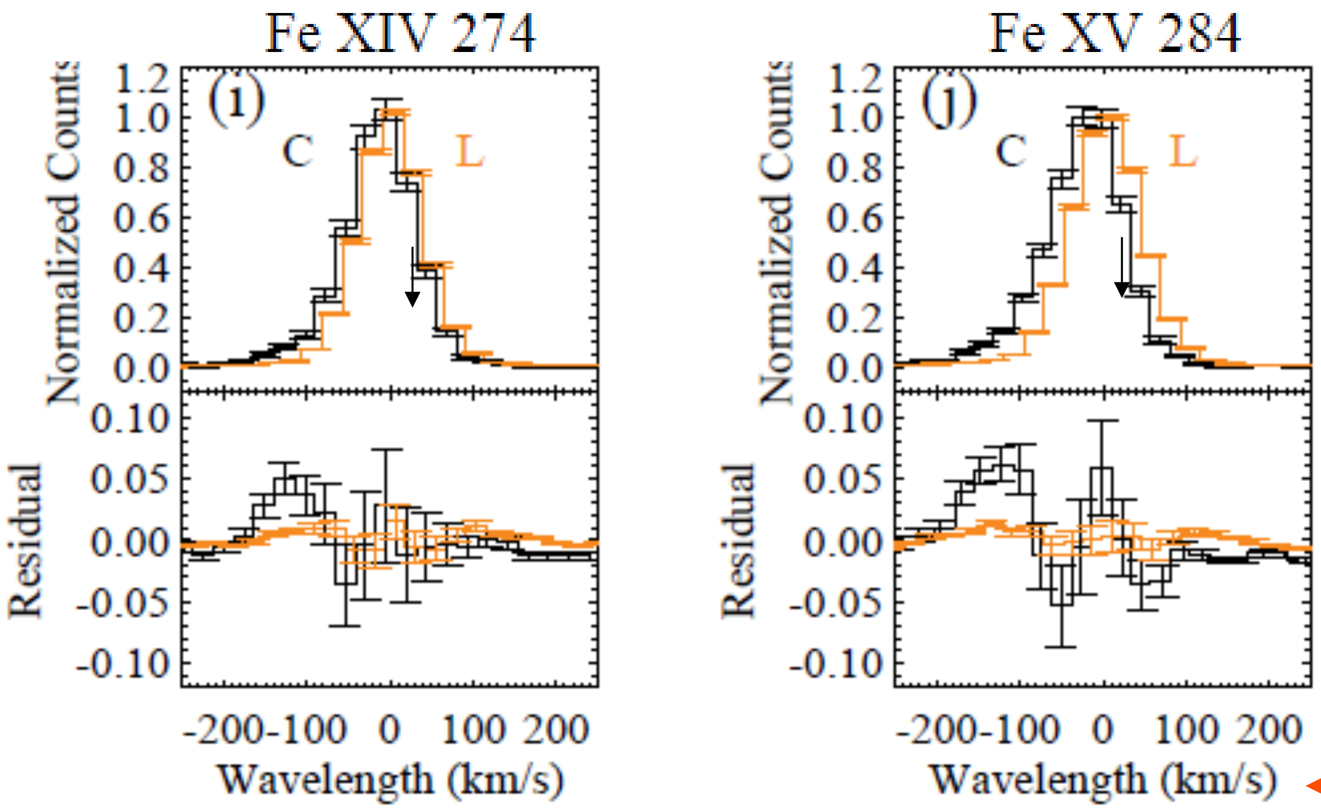

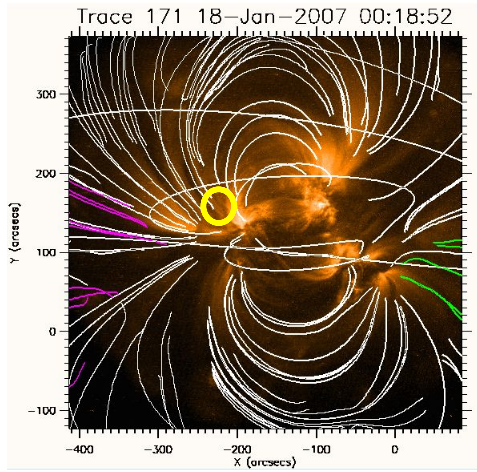

C: disk center

L: limb

$$V_D = \left(\frac{\lambda - \lambda_c}{\lambda_c} \right) c$$

Clearly showing the presence of unresolved high-velocity upflow components that have weaker emission than primary component.

$V_D/\cos\theta$ > 200 km/s ~ V_s

Blue-side Enhanced Line Profile

Line profile
before observations
(solar origin)

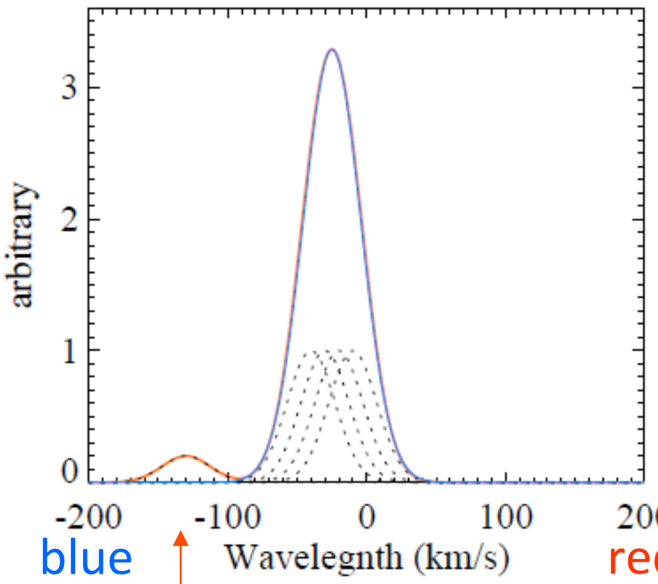

blue red

High velocity upflow

Line profile
by EIS observations
(instrumentally broadened)

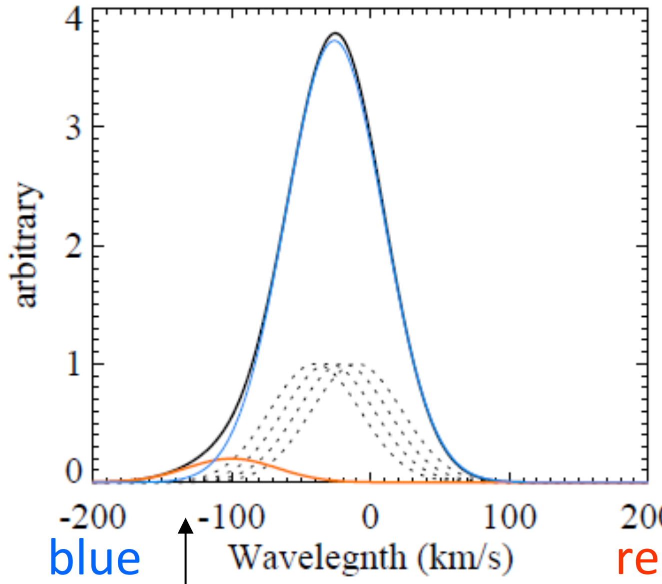

blue red

Blue-side enhancement

Blue lines: Gaussian-fitted line

Thermal energy of high-velocity component within EIS sampling (1 arcsec) unit

- Emission measure $n^2 l = 2.6\times10^{26}$ cm^{-5}
- Volume $V = (725\times10^5 \text{ cm})^3$
  - Width $w = 725\times10^5$ cm
  - Line of sight length $l = 725\times10^5$ cm
- $n = 1.9\times10^9$ cm^{-3}
- $T \sim 1.8\times10^6$ K for Fe XIV 274 observation
- $3nkTV = 5.4\times10^{23}$ erg ~ nanoflare energy

Comparison with a 1D model

Suggestion from numerical simulations

- Antolin et al. (2008)
  - Heating by nanoflare energy input

    1D simulation, L=100 Mm,nanoflare: l=1000 km

    - Uniform heating along a loop
      - V_{max} < 40 km/s、no fast flows
      - V_{mean} ~5 km/s

    EIS observations prefer

    - Footpoint concentrated heating
      - V_{max} > 200 km/s fast flows at footpoints
      - V_{mean} ~15 km/s

    Hara (2009)
  - Heating by torsional Alfven wave through mode conversion
    - Nearly uniform heating over a loop
      - V_{max} > 200 km/s fast flows over a loop
      - V_{mean} ~50 km/s

Frequency distribution on Doppler vel. at disk center

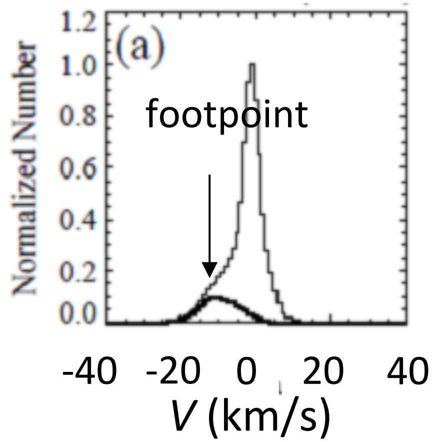

Line profile from a simulation result

Nanoflare simulation (footpoint heating)
[nanoflare input at 2 -12 Mm height

Antolin et al. (2008)

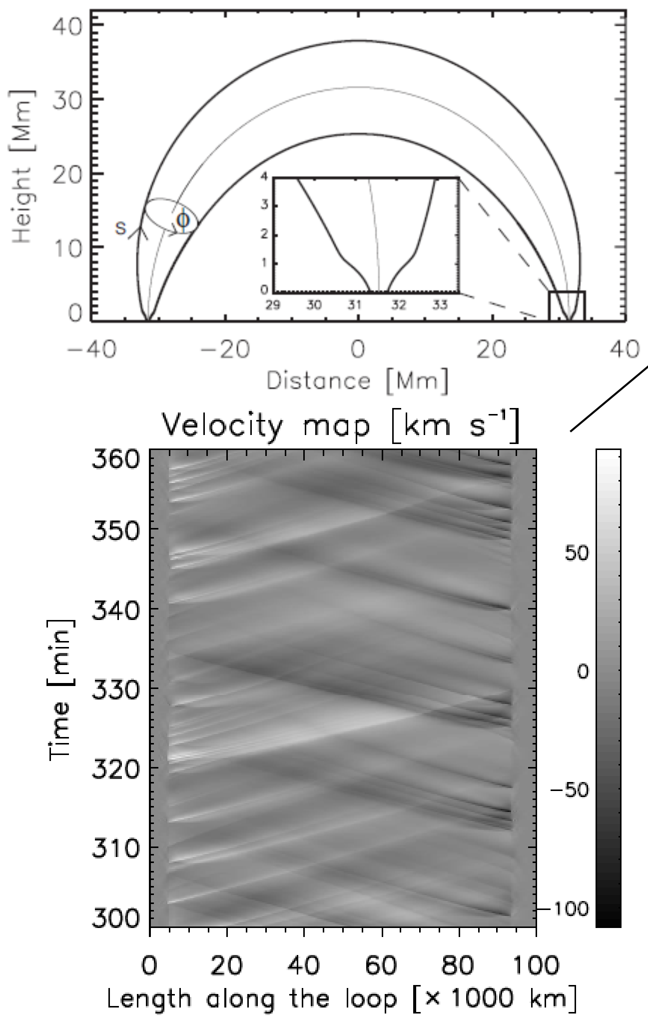

$N(z)$
$T(z)$
$V(z)$

Temporal average for the case of multiple strands

Calculate emission-line profile

Expected line profile
Fe XV 284

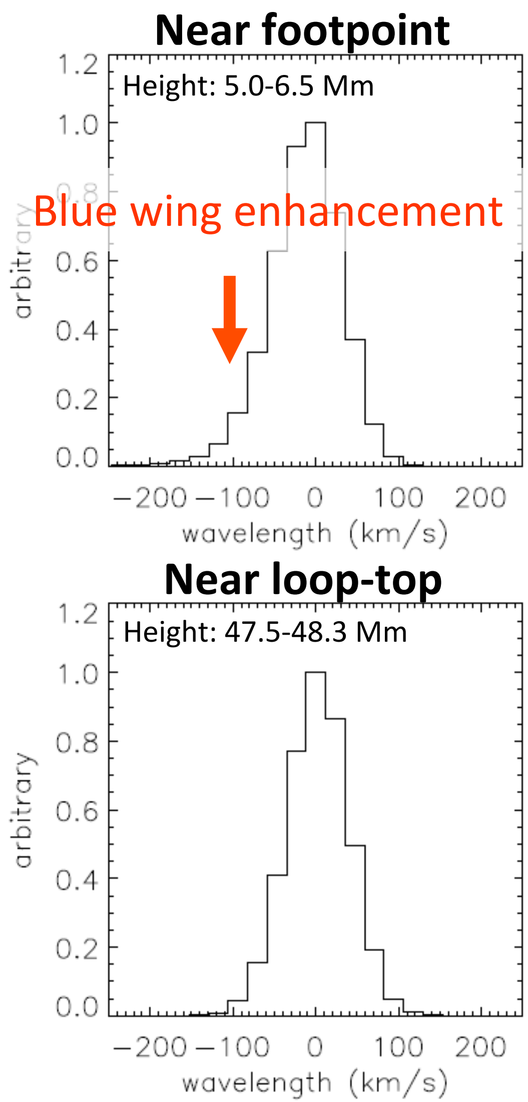

high-speed component
- understanding in 2008 -

- High velocity in the corona:
  - impulsive energy deposition
- Location of high speed component: [near footpoints]
  - Energy deposition is at low coronal height.

  ➔ understood so from comparison with simple model calculations

  ❖Hara+'s idea was misunderstood by referring a blue-wing enhancement expected from a nanoflare model (Patsourakos & Kimchuk 2006), which predicts a high-speed component over the loop.
- Low emission:
  - Scale of energy deposition may be smaller than the EIS spatial resolution.
- Intermittency:
  - < 25 min only confirmed from slow EIS raster data covering AR plage.
  - Frequent occurrence was found later by sit-and stare observations.

Blue-Red asymmetry

Line asymmetry map from EIS

Log scale

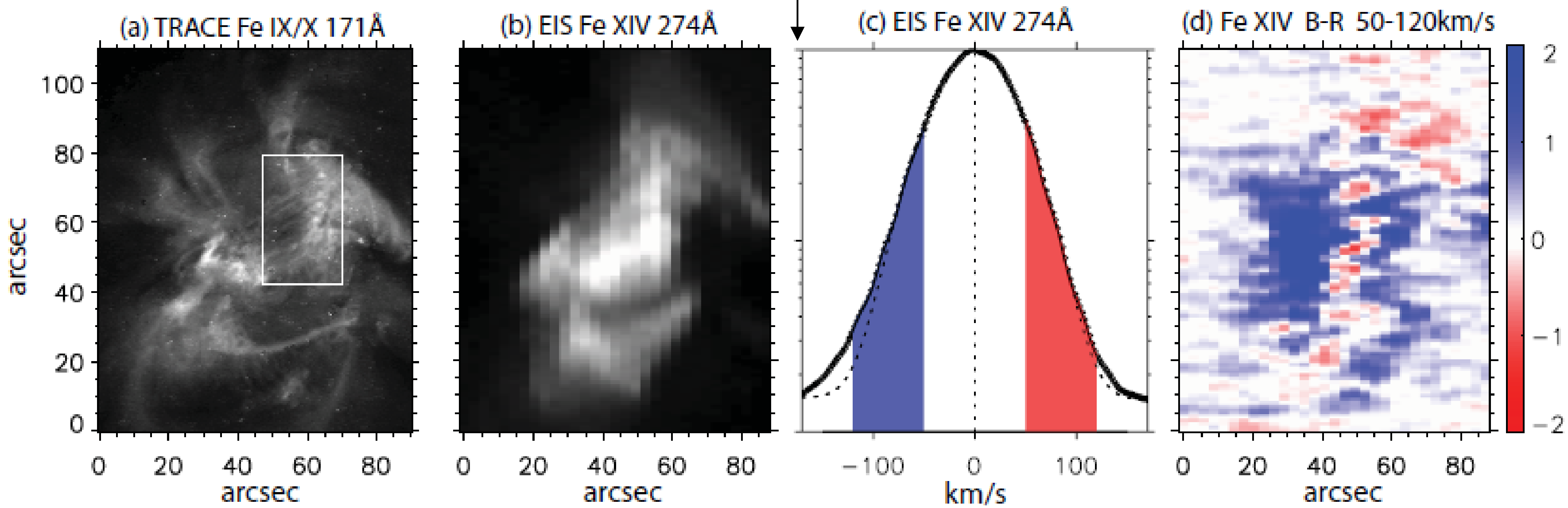

De Pontieu et al. (2009)

by internal
pixel interpolation

Signature of
fast flows
in moss region

Relation to chromospheric activity

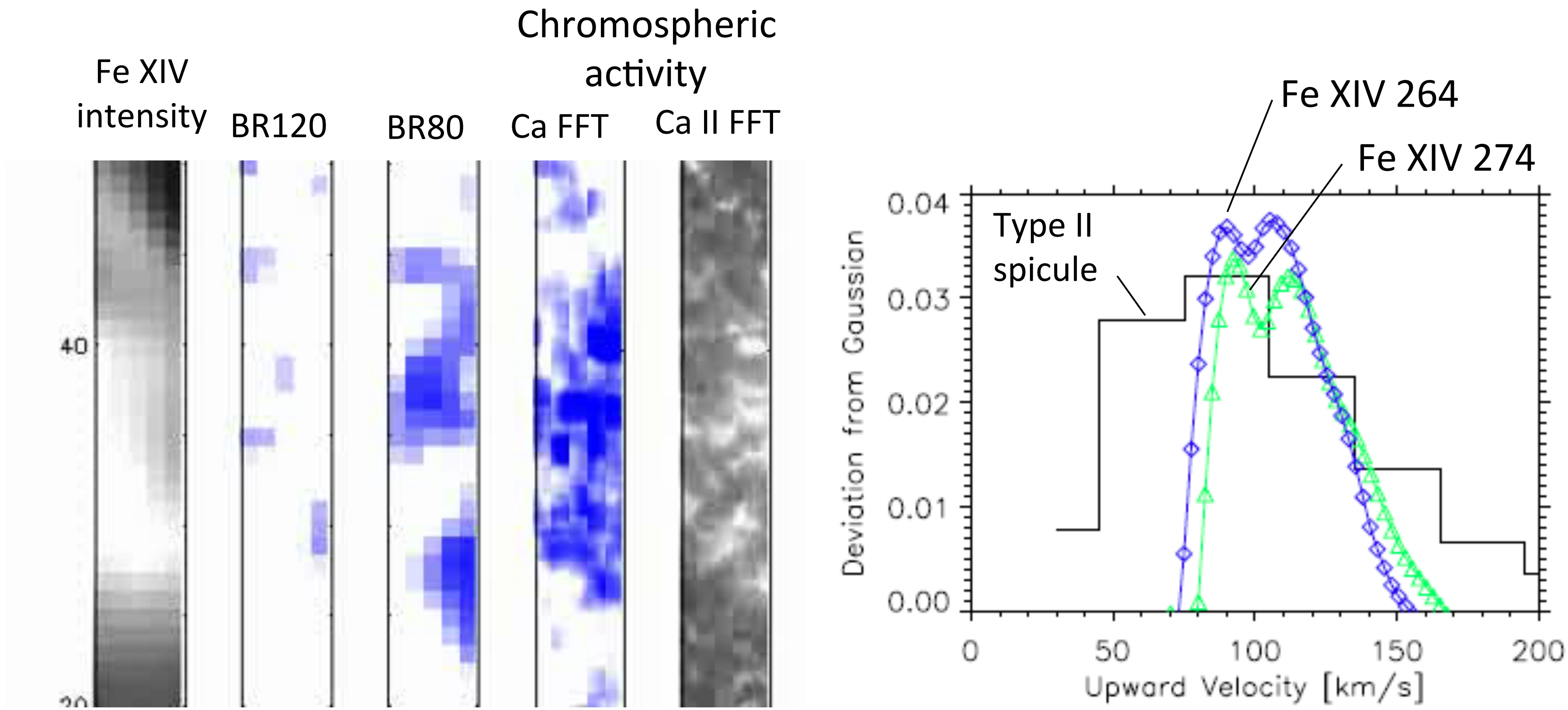

De Pontieu et al. (2009)

'A significant part of the heating and energizing of the corona occurs at chromospheric heights, in association with chromospheric jets.'

Multiple Doppler components

- Double Gaussian fitting by Bryan et al. (2010), Peter (2010), Tian et al. (2011) basically confirms the presence of high-speed component at the blue wing.
- The nature of the high-speed component is shown below:
  both double Gaussian and RB-asymmetry analysis are shown from Tian+2011.

1: core component, 2: wing component

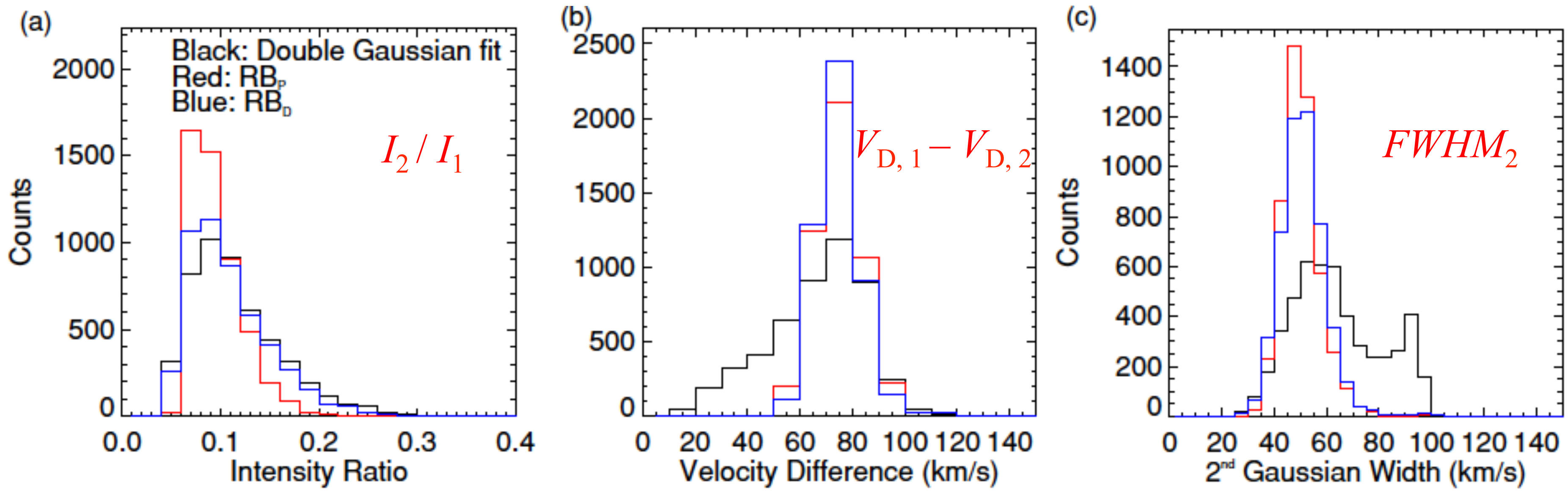

Tian et al. 2011, ApJ, 738, 18

Position of secondary component

Hara+2008, ApJ, 678, L67

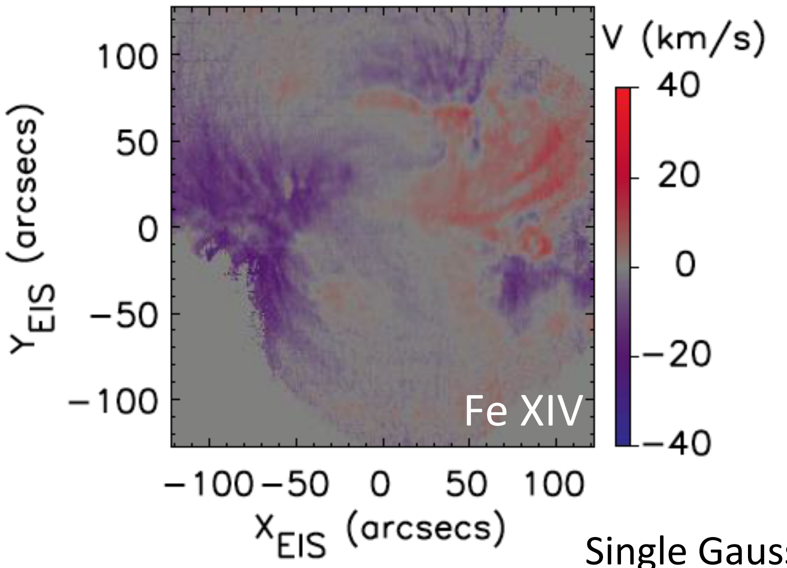

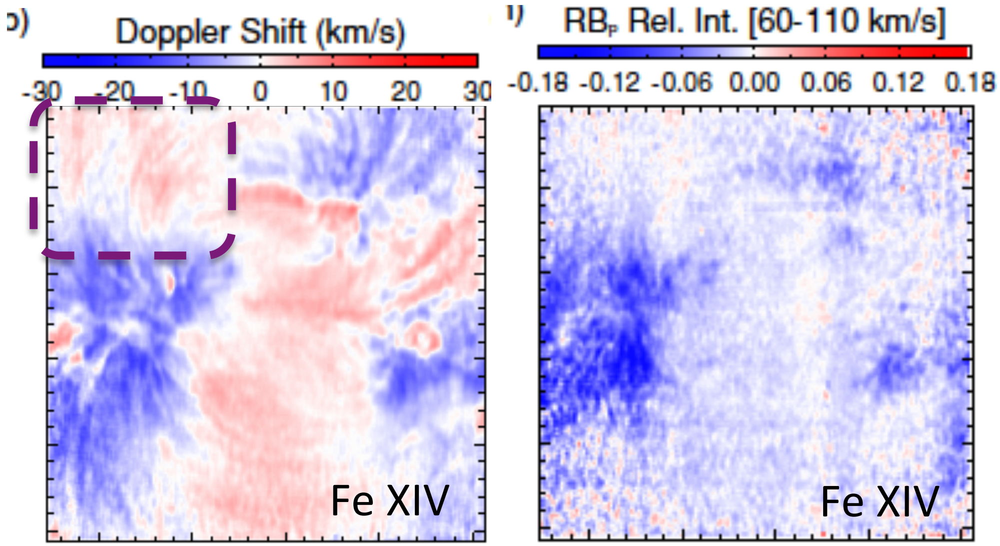

Tian+2011, ApJ, 738, 18

Artifact

Peter 2010,
AA, 521, A51

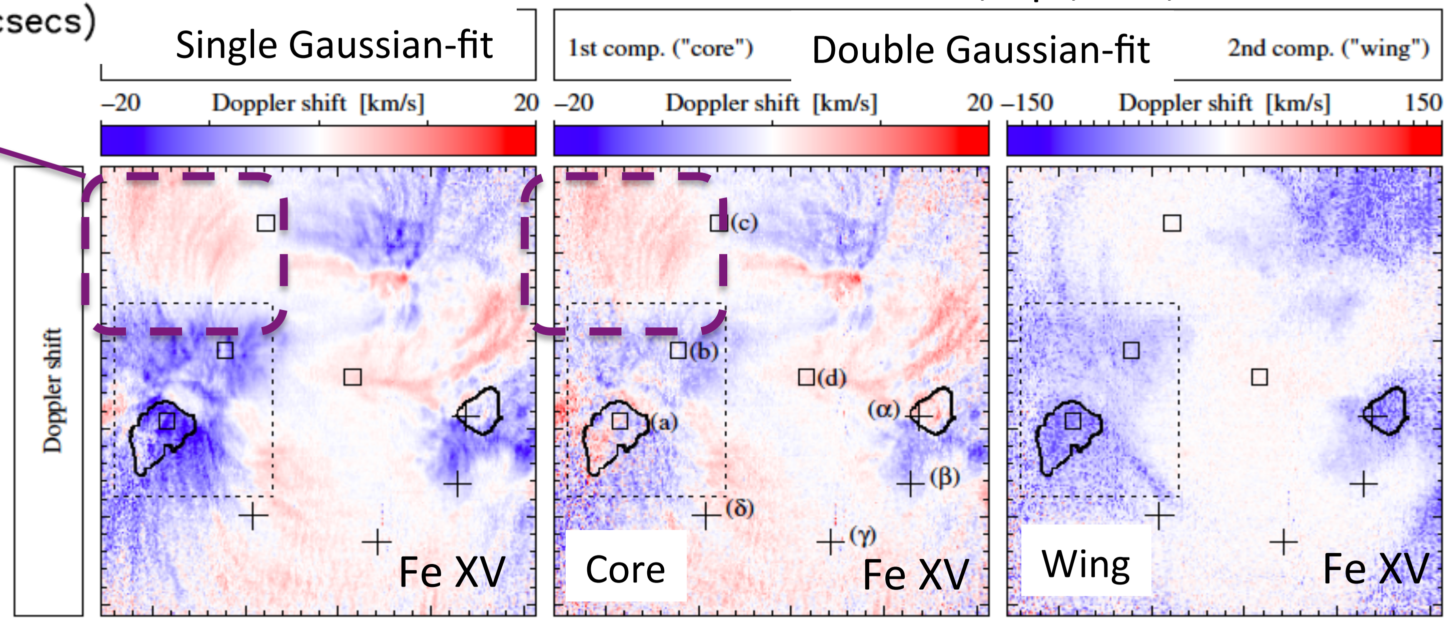

What magnetic structures associated with the high speed flow?

Interpretation by magnetic reconnection for unresolved fast flows

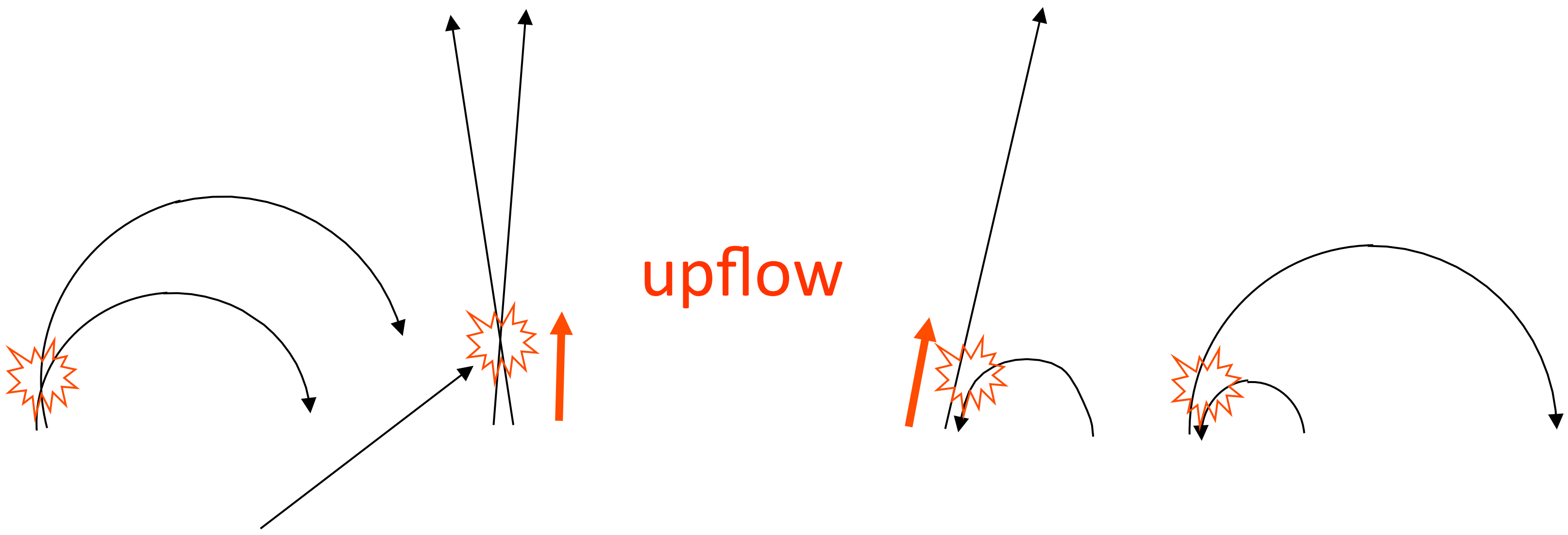

- Local Alfven speed in the reconnection region will be much smaller than so-called coronal Alfven speed.
- Dominant flow direction will be along the guide field.

What magnetic structures are associated with the high-speed flows in AR?

Outflow from Edge of Active Region

- Apparent fast outflow structure has been found at the edge of active region from *Hinode* X-ray observations in the corona.
- Hinode spectroscopic coronal observations support the fast flow as real outflow.

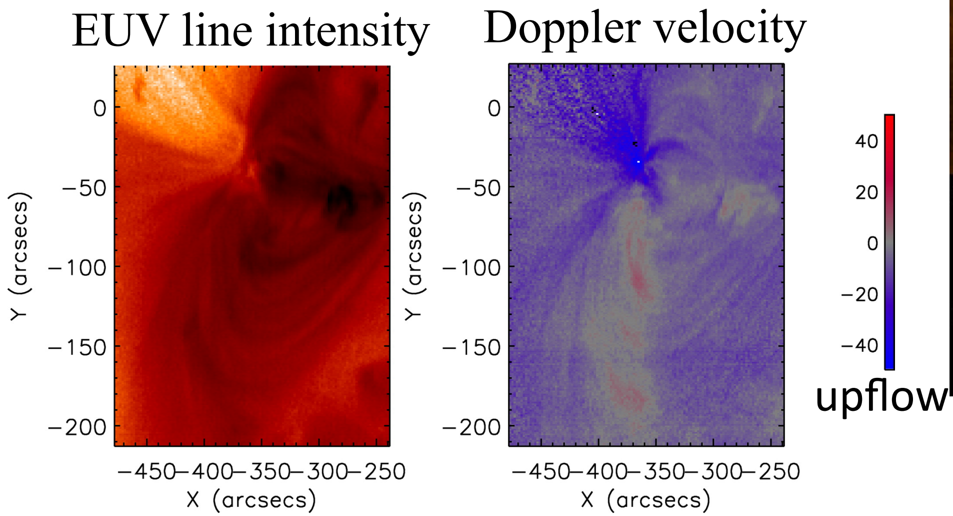

Harra et al. 2008, ApJ, 676,L147

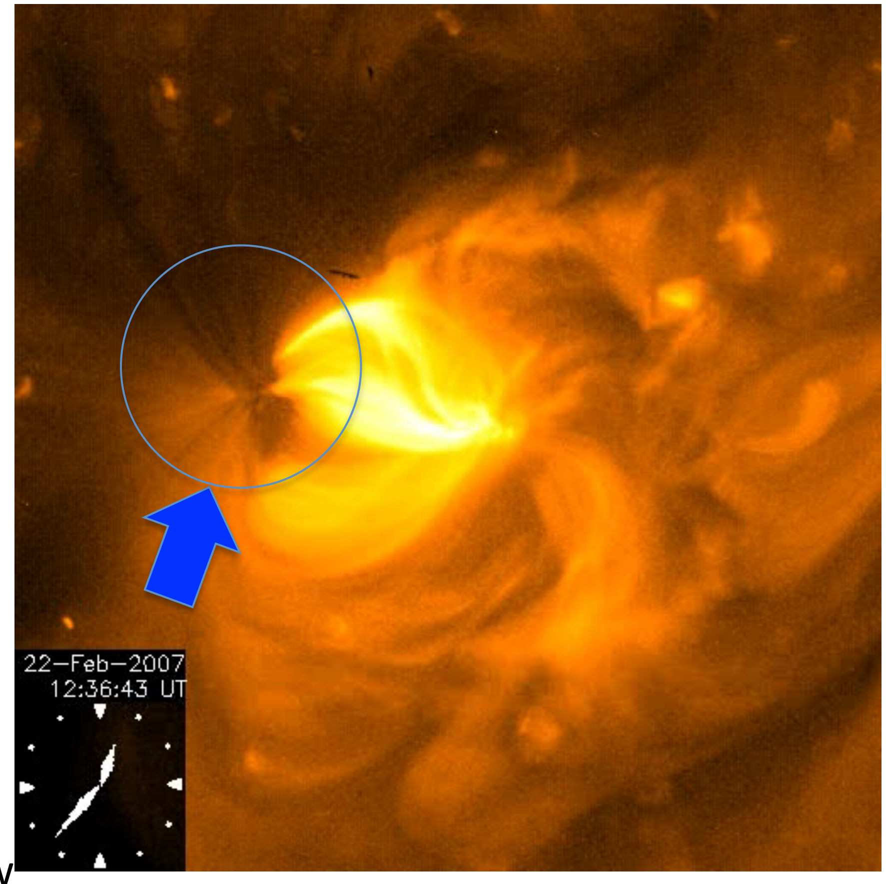

Sakao et al. 2007, Science, 318, 1585

Outflow from Edge of Active Region

- Magnetic field in the source region of the outflow is connected to be interplanetary space.
- It is considered to be the source of slow solar wind.

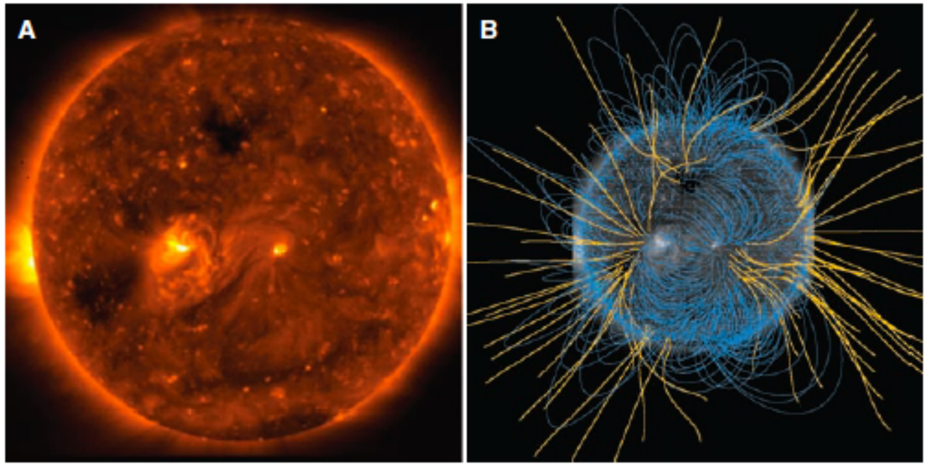

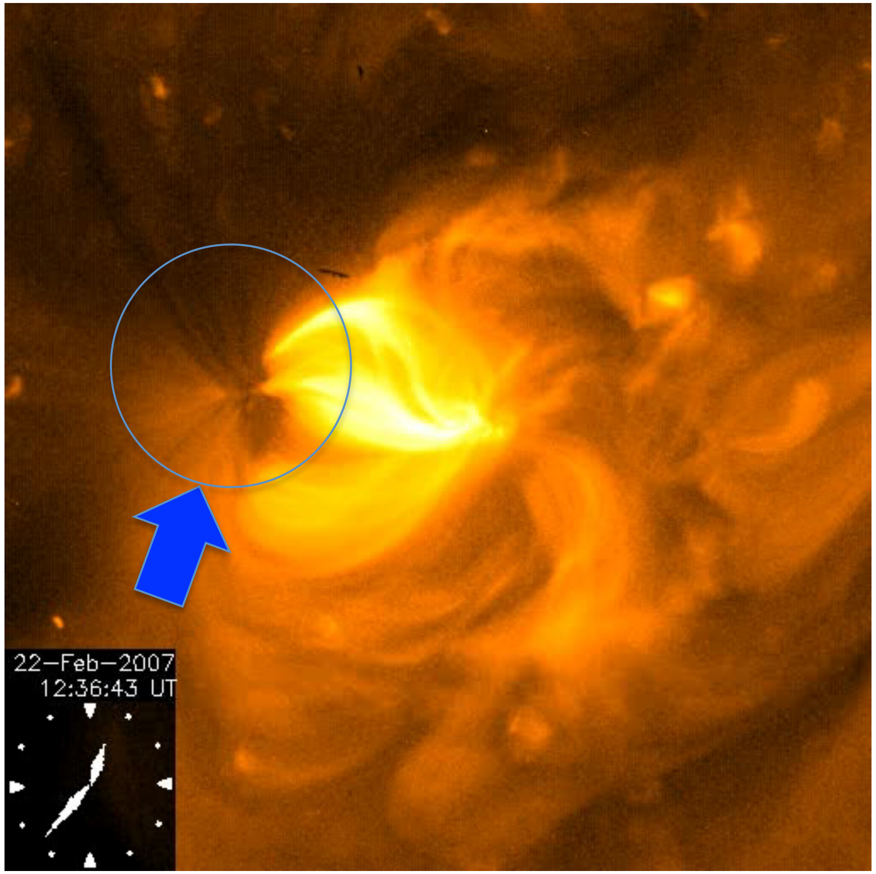

Sakao et al. 2007, Science, 318, 1585

Quasi-separatrix layers (QSLs)

Fe XII line intensity

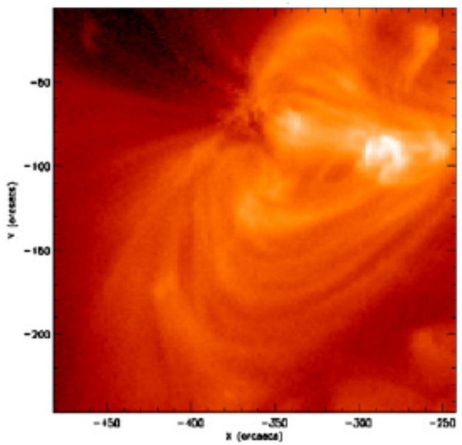

Fe XII Doppler velocity
with MDI *B* contours (50G)

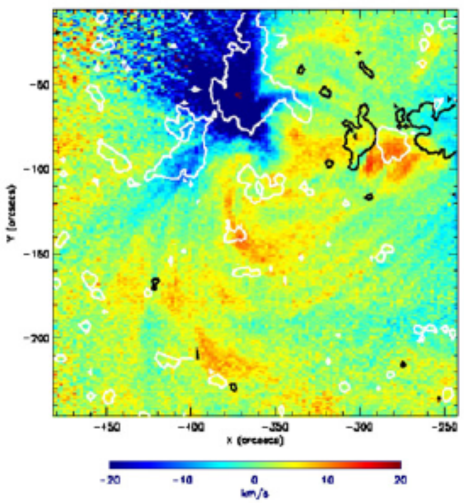

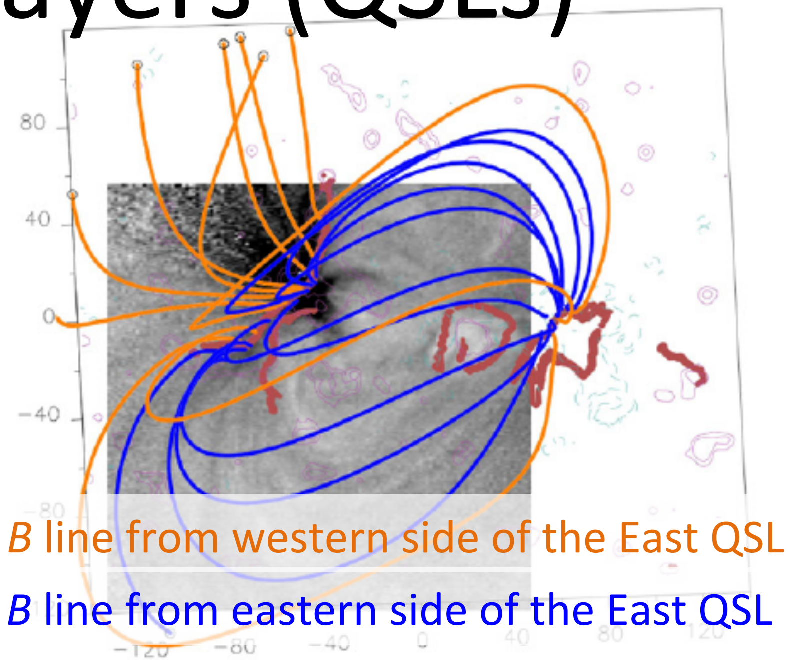

'The outflows originate from specific locations of the magnetic topology where field lines display strong gradients of magnetic connectivity, namely quasi-separatrix layers (QSLs), or in the limit of infinitely thin QSLs, separatrices.'

➔Magnetic reconnection at QSL is the driver of outflows

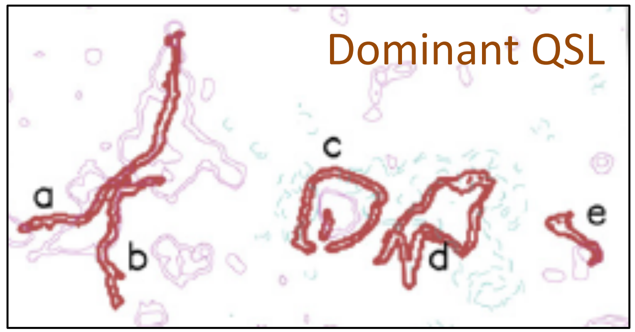

Baker et al. 2009, ApJ, 705, 926

Related work: van Driel-Gesztelyi et al. 2012, Solar Phys., 281, 237
Demouline et al. 2013, Solar Phys., 283, 341

Temporal scale of high-speed component

Quasi-periodic upflow

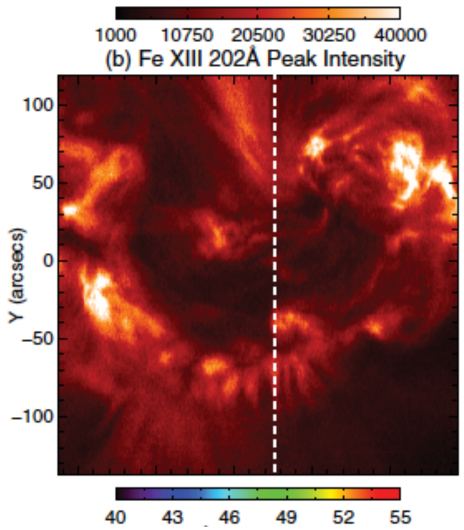

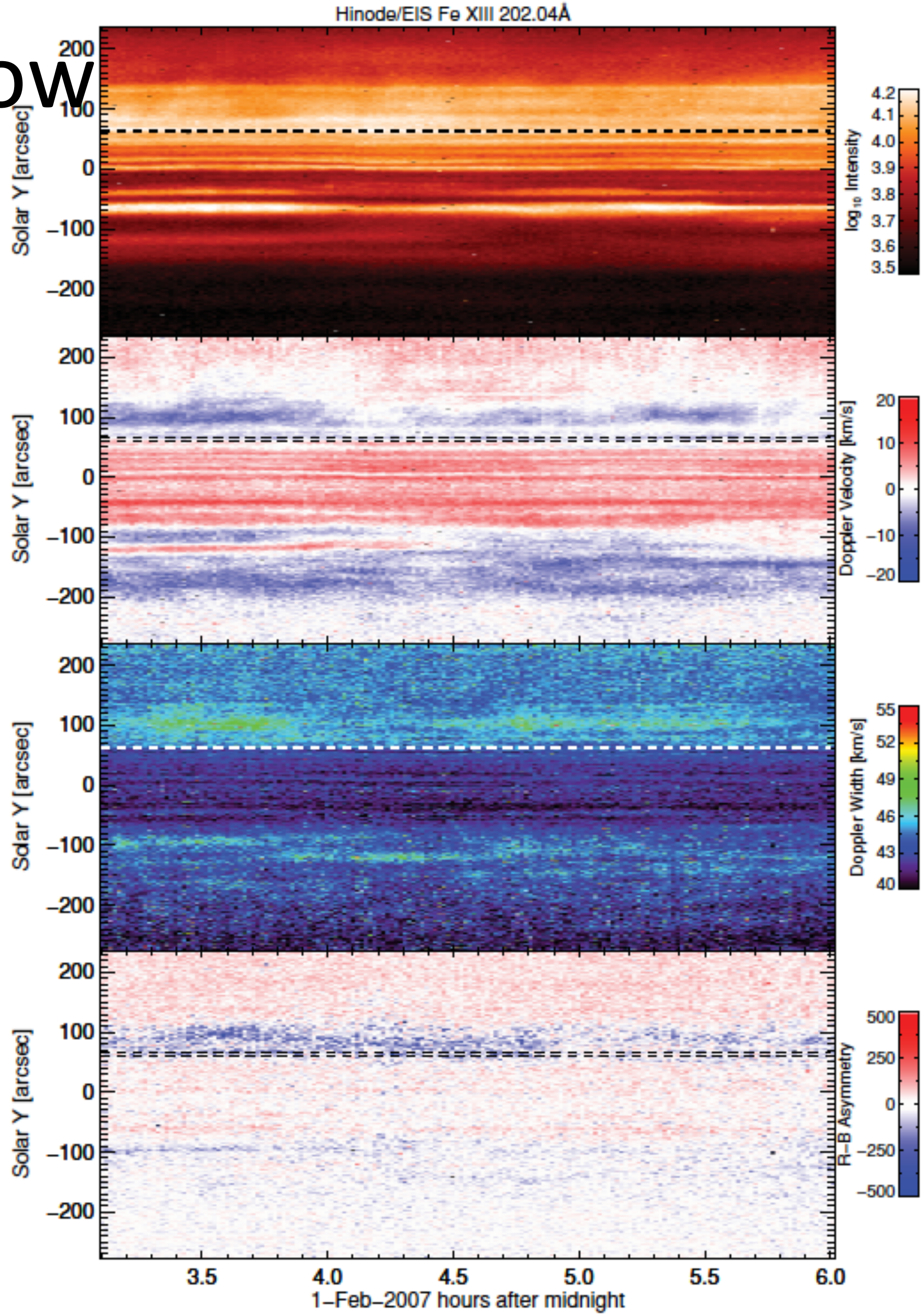

De Pontieu & McIntosh 2010, ApJ, 722, 1013

Quasi-periodic upflow

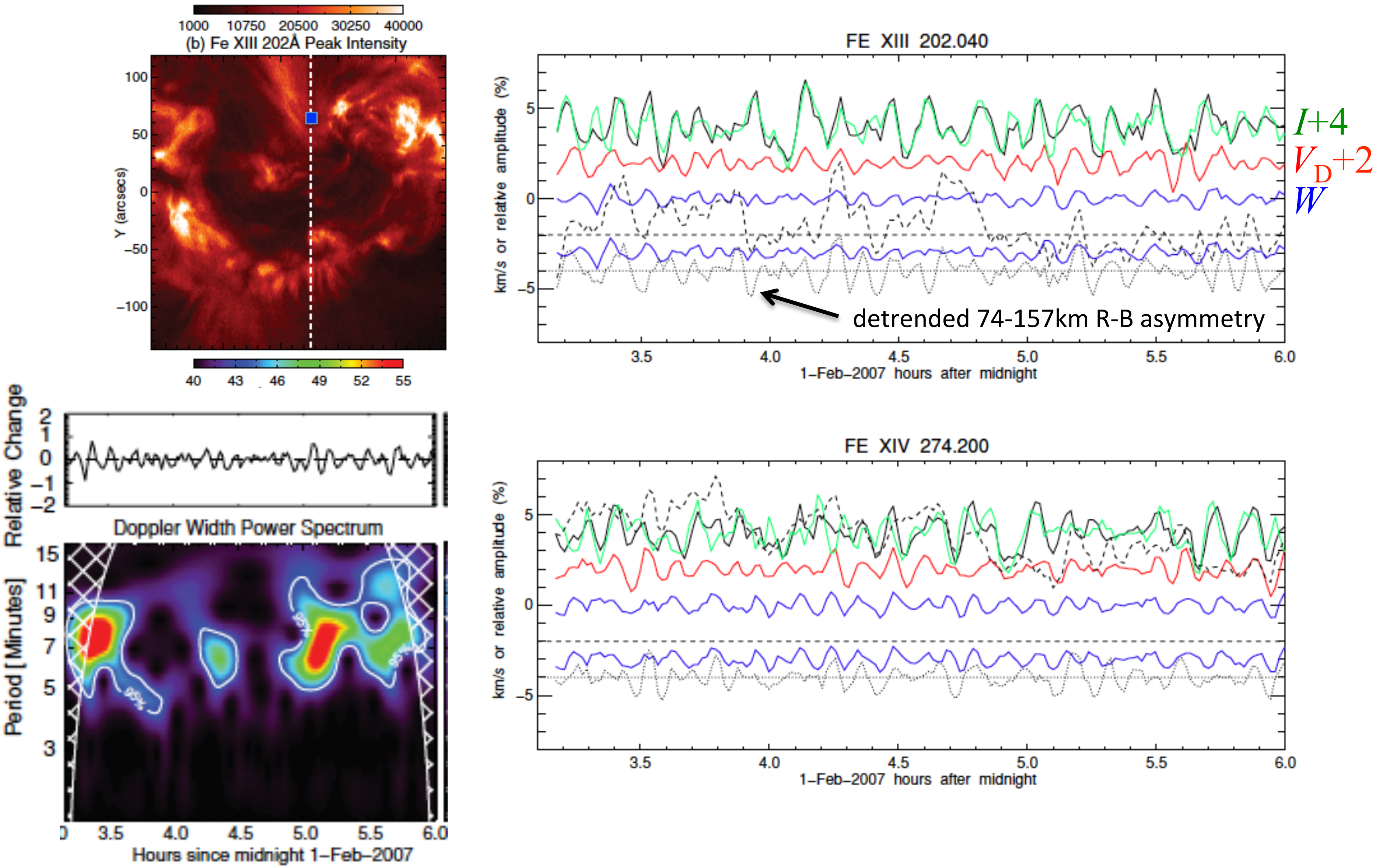

De Pontieu & McIntosh 2010, ApJ, 722, 1013

Quasi-periodic upflow

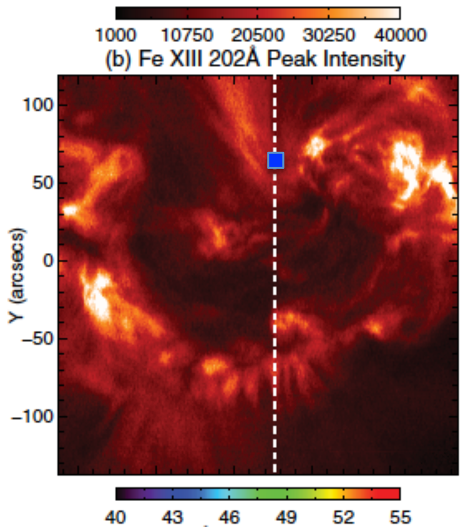

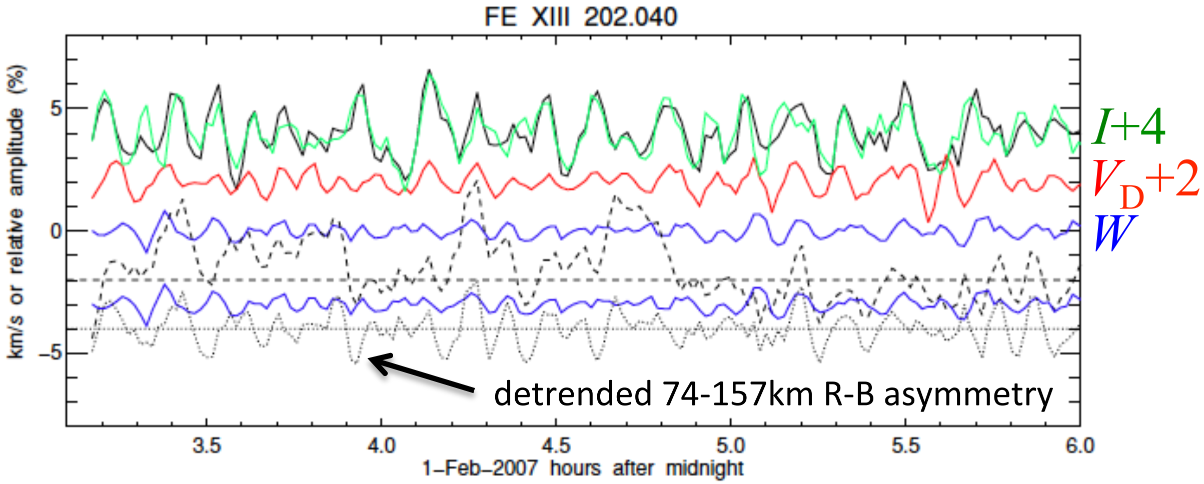

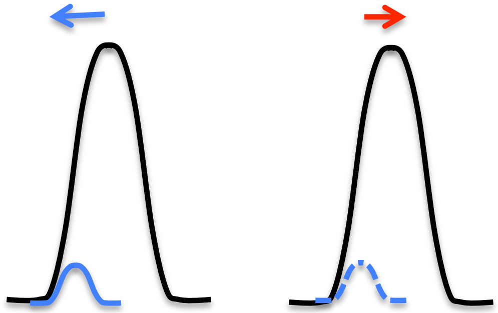

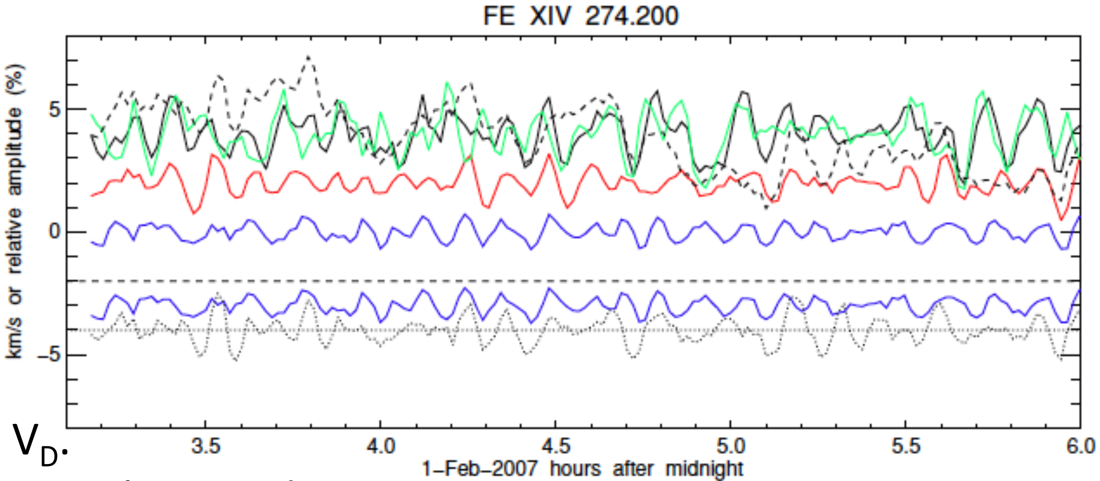

Another interpretation of
in-phase relation between I and V_D.
Normally interpreted as propagating slow-mode waves.

De Pontieu & McIntosh 2010, ApJ, 722, 1013

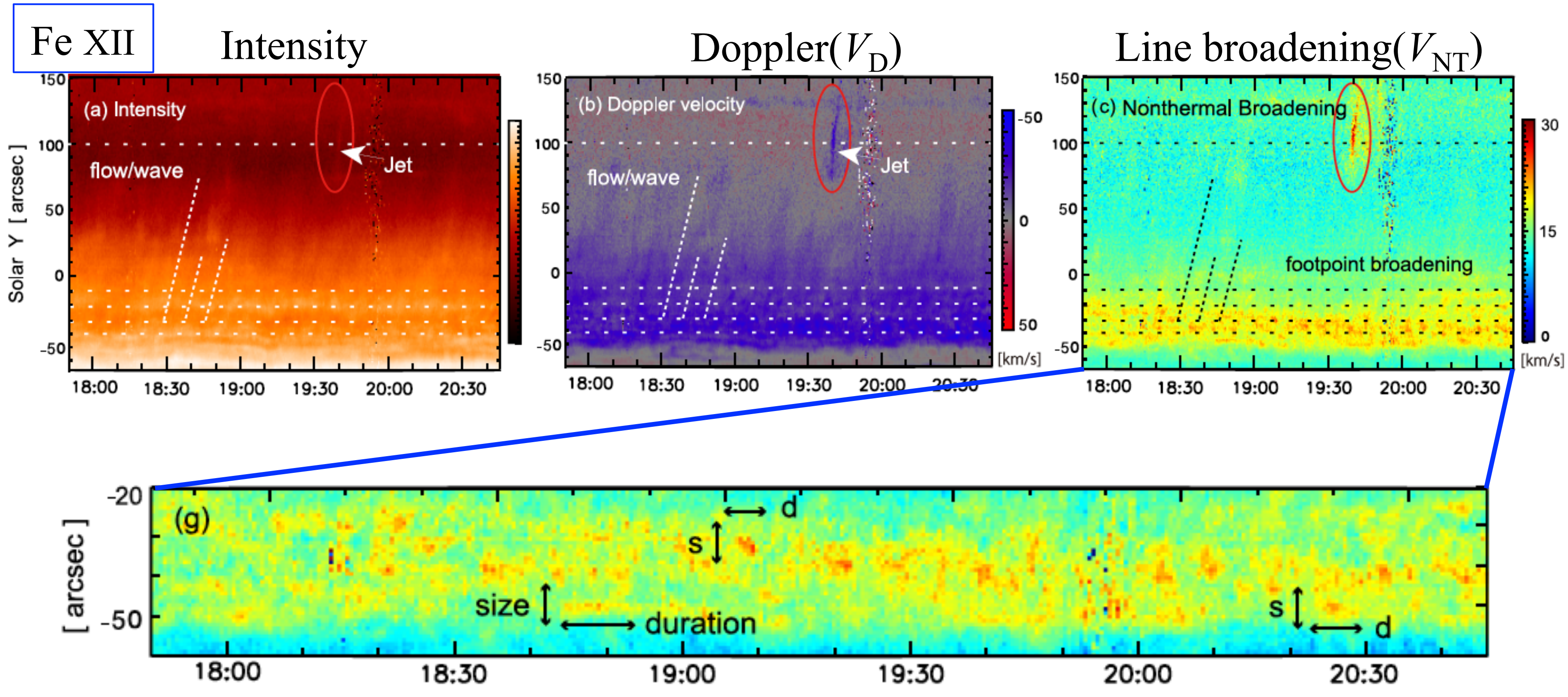

(Observation time: 17:50 -20:45 UT on 2007 February 20)

- Short duration (~1 min) V_{NT} events frequently occur at the base of the corona.
- The upflows and upward propagating disturbance appear to start there.
- The line profile that is in the high corona is very symmetric. No fast V_D component is identified in the high corona.

Nishizuka & Hara 2011, ApJ, 737, L43

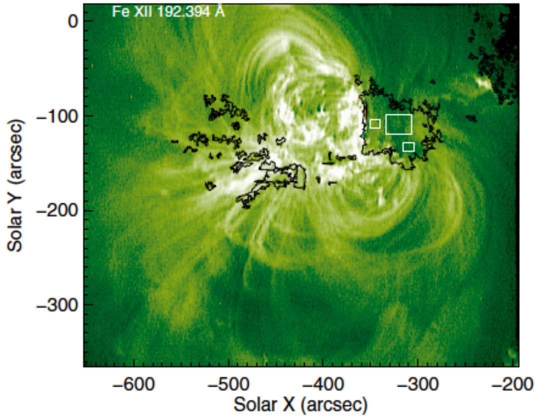

T_e dependence
in outflow region

Brooks & Warren 2012, ApJ, 760, L5

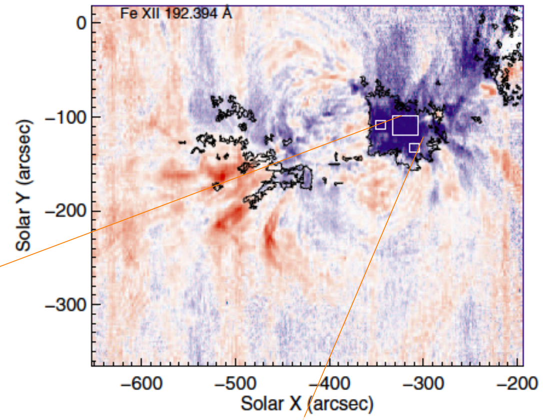

- The asymmetries are dependent on temperature, and are clearer and stronger in coronal lines.

28"× 21" area in the upflow region

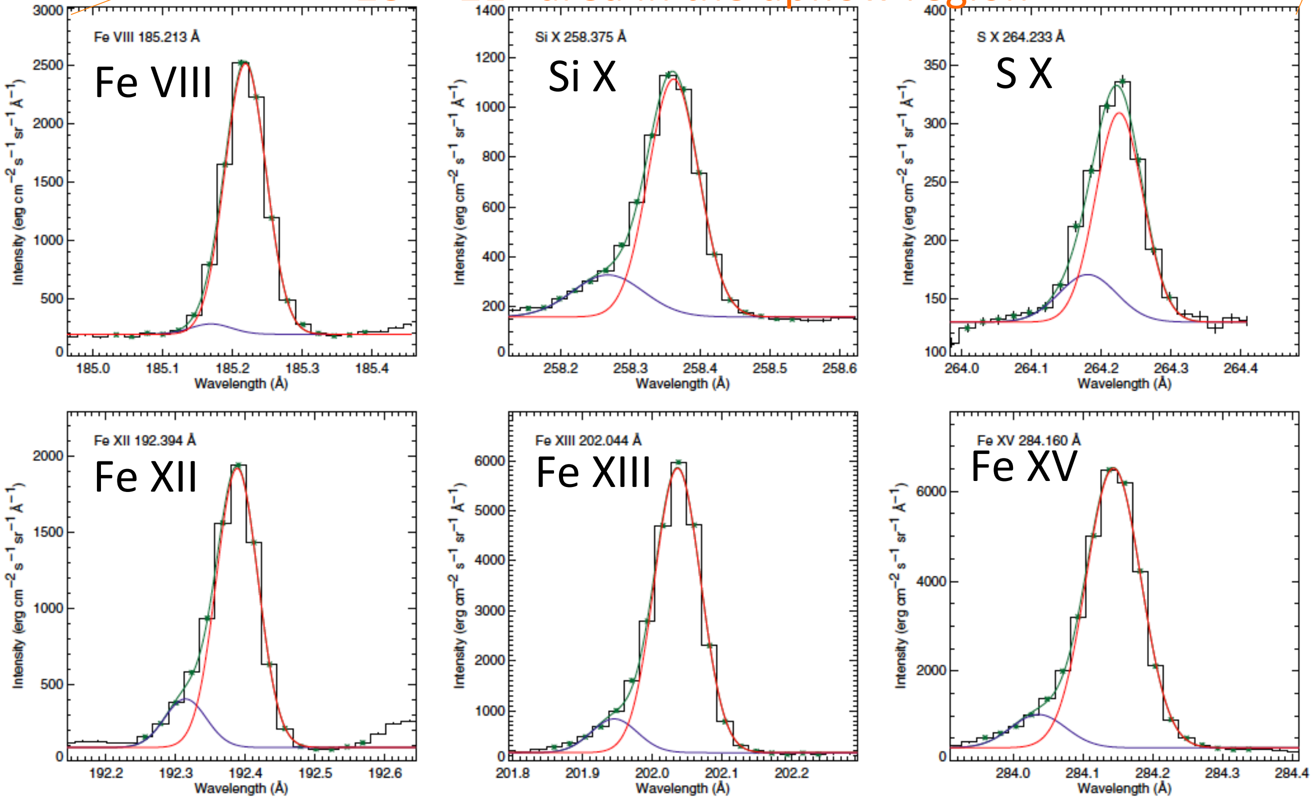

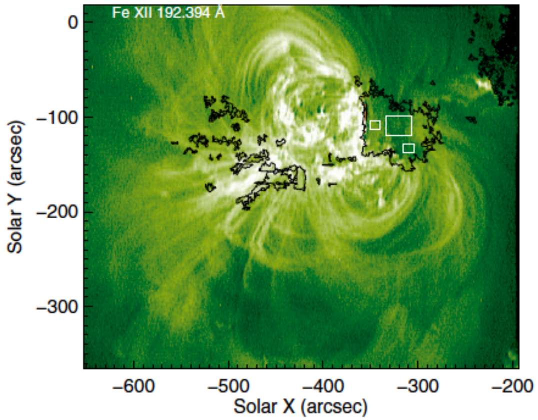

T_e dependence in outflow region

Brooks & Warren 2012, ApJ, 760, L5

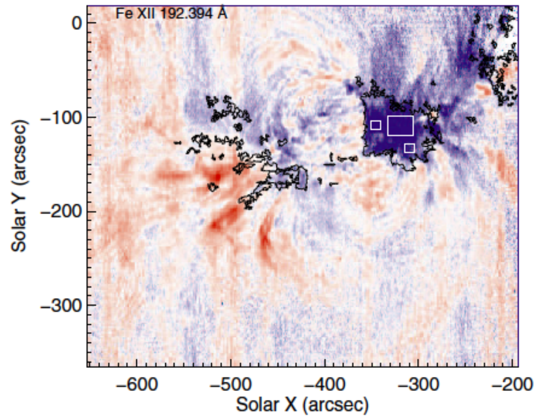

- A faint enhancement In the blue wing appear for T_e > 0.6 MK.
- FIP bias of the faint fast component: 3-5
  - The high-speed component may contribute to the slow-speed wind.
    (see Brooks & Warren 2011, ApJ, 727, L13 for the primary component.)

- The high-speed plasma producing the blue asymmetry is in a coronal origin in the outflow region.

  How about at the loop footpoint?

R-B asymmetry in 3D modeling

Martinez-Sykora et al. 2011, ApJ, 732, 84

- R-B asymmetry is found at the footpoint of coronal loops in the Oslo 3D MHD simulation.
- But it is an order of magnitude smaller than what we observe with EIS. ➔Difficult to detect that level from EIS observations.

- R-B asymmetry in the model is more prominent in TR that in the corona.
- EIS observations in the outflow region show that the asymmetry is stronger in the corona (Brooks & Warren 2012).

- Viggo may explain this issue in his presentation later.

Summary

- *Hinode* EIS has revealed flow structures in active regions.
- Upflow structures along coronal loops, as response of coronal heating, have been found.
- High-speed upflows (V_D~50-100 km/s) are concentrated near the footpoints of coronal loops, which is evidence for a direct signature of footpoint heating.
- High-speed upflows appear in unipolar plage regions and are located at QSL where component reconnection may occur. Relation between local magnetic structures and coronal event is not well known.
- PD appears to be associated with the events at the loop footpoint.